biosensors

MDPI

Review

Application of Nanozymes in Environmental Monitoring, Management, and Protection

Miaomiao Wang [1,2], Ping Zhu [1,2], Shuge Liu [1,2], Yating Chen [1,2], Dongxin Liang [1], Yage Liu [1,2], Wei Chen [1,2,*], Liping Du [1,2,*] and Chunsheng Wu [1,2,*]

[1] Institute of Medical Engineering, Department of Biophysics, School of Basic Medical Sciences, Health Science Center, Xi'an Jiaotong University, Xi'an 710061, China
[2] Key Laboratory of Environment and Genes Related to Diseases, Xi'an Jiaotong University, Ministry of Education of China, Xi'an 710061, China
* Correspondence: weiwcchen@xjtu.edu.cn (W.C.); duliping@xjtu.edu.cn (L.D.); wuchunsheng@xjtu.edu.cn (C.W.)

Abstract: Nanozymes are nanomaterials with enzyme-like activity, possessing the unique properties of nanomaterials and natural enzyme-like catalytic functions. Nanozymes are catalytically active, stable, tunable, recyclable, and versatile. Therefore, increasing attention has been paid in the fields of environmental science and life sciences. In this review, we focused on the most recent applications of nanozymes for environmental monitoring, environmental management, and environmental protection. We firstly introduce the tuning catalytic activity of nanozymes according to some crucial factors such as size and shape, composition and doping, and surface coating. Then, the application of nanozymes in environmental fields are introduced in detail. Nanozymes can not only be used to detect inorganic ions, molecules, organics, and foodborne pathogenic bacteria but are also involved in the degradation of phenolic compounds, dyes, and antibiotics. The capability of nanozymes was also reported for assisting air purification, constructing biofuel cells, and application in marine antibacterial fouling removal. Finally, the current challenges and future trends of nanozymes toward environmental fields are proposed and discussed.

Keywords: nanozyme; sensing; monitoring; environmental pollutant; catalytic activity

Citation: Wang, M.; Zhu, P.; Liu, S.; Chen, Y.; Liang, D.; Liu, Y.; Chen, W.; Du, L.; Wu, C. Application of Nanozymes in Environmental Monitoring, Management, and Protection. *Biosensors* **2023**, *13*, 314. https://doi.org/10.3390/bios13030314

Received: 4 January 2023
Revised: 10 February 2023
Accepted: 16 February 2023
Published: 24 February 2023

1. Introduction

Most life activities in nature involve enzymes. Natural enzymes are macromolecular biocatalysts composed of most proteins and a few nucleic acids that run through the metabolism of life [1]. They have high catalytic efficiency, good substrate specificity, and biocompatibility [2]. Therefore, they are widely used in various fields, including disease diagnosis, clinical treatment, agricultural engineering, paper and leather, textile industry, and food processing. However, most natural enzymes are easy to inactivate or their activities are inhibited under nonphysiological conditions, which severely limits the wide application of enzymes. In addition, enzymes also have defects such as storage stability and recovery difficulties, complex production as well as purification processes, and high costs [3,4]. With the rapid development of nanoscience and life science, simulating the structure and catalytic activity of natural enzymes to construct substitute products has gradually become a new direction in which to expand the application of natural enzymes.

The term "artificial enzymes" was coined by Ronald Breslow for enzyme mimics. An "artificial enzyme" combines a metal catalytic group and a hydrophobic binding cavity [5]. In 2004, Scrimin and his colleagues created the term "nanozyme" and used gold nanoparticles functionalized by triazetidine as the catalyst for the transphosphorylation reaction [6]. In 2007, Yan's team found that magnetic nanoparticles (Fe_3O_4 MNPs) have a catalytic activity similar to horseradish peroxidase (HRP), indicating that some inorganic nanoparticles can also have peroxidase-like properties [7]. In 2013, Wei and Wang used the term

"nanozyme" to describe some nanoscale materials with enzyme-like characteristics, namely, nanozyme is a kind of nanomaterial with similar natural enzyme catalytic activity and enzymatic reaction kinetics [8]. In the ten years since then, nanozyme experienced a period of rapid development and application in various fields. Based on advanced nanotechnology, a variety of nanozymes with catalytic activity comparable to that of natural enzymes have been explored. Compared with natural enzyme, nanozyme has the following obvious advantages: (I) High stability: inorganic nanomaterials are less fragile than natural enzymes, which enables the use of nanozymes under a wide range of pH (3–12) and temperature (4–90 °C) conditions. In contrast, natural enzymes are usually inactivated under extreme pH and temperature conditions. (II) Low cost: the production process of enzymes is usually complex and expensive, while inorganic nanomaterials are easy to produce, with high efficiency and low cost. (III) Recycling: Nanozymes are recyclable, and there is no substantial loss of catalytic activity in subsequent cycles. (IV) Easily multifunctional: Nanozymes have sufficient surface area to allow them to be coupled with multiple ligands to achieve multifunctionability [9]. (V) High catalytic activity: The level of activity is comparable to that of biological enzymes with the help of advanced nanotechnology. At the same time, a variety of factors influence the level of activity such as size, shape, composition, crystal surface, charge, and hydrophilicity. Although nanozymes have the above advantages, some nanozymes have the disadvantages of toxicity, low specificity, and poor dispersion. During the degradation and protection of environmental pollutants by nanozymes, nanozymes inevitably contact with water, animals and plants, soil, and air. Therefore, the safety of nanozymes is crucial. For example, some heavy metal nanozymes (Au, Cu, Ce, Fe, etc.) will be absorbed into soil and water, causing ecological pollution [10]. The continuous enrichment of heavy metals will eventually endanger human health through the food chain. In addition, graphene, quantum dots, copper–carbon dots and other nanomaterials have their own toxicity, and their dispersion will be strengthened during trial, which will make them more easily absorbed by aquatic plants and water bodies [11]. Toxicity can be reduced by reducing the size of nanozyme [12]. In addition, we can control the surface charge of nanozyme to regulate its permeability to cells in the human body [13]. The metal core is the source of toxicity, so it can be prevented from leakage by mixing other metal ions and chemical sealing [14,15].

The International Enzyme Commission (I.E.C.) specifies that natural enzymes can be classified into six categories by the enzymatic reaction as oxidoreductases, hydrolases, isomerases, lyases, ligases, transferases. Since nanozymes are a class of nanomaterials that mimic the catalytic activity and enzyme kinetic characteristics of natural enzymes, the categories also similar to that of natural enzymes could divide nanozymes into the following six categories: redox nanozyme, hydrolyzing nanozyme, lytic nanozyme, transfer nanozyme, isomeric nanozyme, and linked nanozyme. Currently, the reported nanozymes are mainly in the redox nanozyme family, whose members are oxidase (OXD) [16], peroxidase (POD) [17], catalase (CAT) [18], and superoxide dismutase (SOD) [19] (Figure 1). Oxidase catalyzes the oxidation of substrates using oxygen as the electron acceptor. Subsequently, O_2 is reduced to water or hydrogen peroxide. Peroxidase nanozyme can catalyze peroxides whose substrate is usually used as an electron donor. In biomedicine, it defends against pathogens and removes the toxicity of reactive oxygen [20]. Catalase often catalyzes H_2O_2 to produce oxygen and water. It is found that many metal materials and even metal oxides have catalase-like activity. Superoxide dismutase disproportionates superoxide radicals into oxygen and hydrogen peroxide and alleviates oxidative stress generated from cell metabolism. There is also a family of hydrolyzing nanozymes including phosphatases [21], nucleases, and proteases. They catalyze the separation of phosphate groups and the hydrolysis of phosphate diester bonds and peptide bonds. The family of lytic nanozyme comprises the carbonic anhydrase [19]. Nanozymes mostly catalyze the optical signal transmission of chromogenic substrates, so that other three types of nanozymes are rarely reported. It is hoped that the design of nanozymes can break through more types and functions limitations.

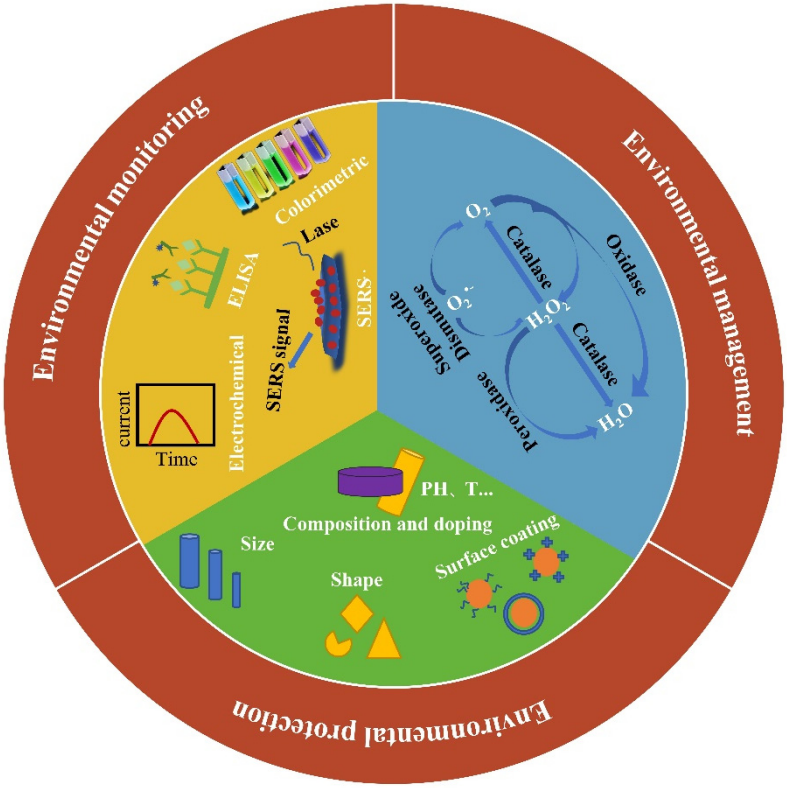

Figure 1. Nanozyme as a promising tool from environmental monitoring and environmental management to environmental protection.

The reported nanozymes can be classified into four categories according to the materials, such as metal-based, metal oxide-based, carbon-based, MOF-based, and other material-based. Currently reported carbon-based nanozymes include fullerenes, carbon nanotubes (CNTs), graphene, graphene oxide (GO), carbon dots (CDS), graphitic quantum dots (GQDS), and carbon nitrides [22]. Because of their special electronic and geometric properties, they can mimic the catalytic center of natural enzymes and possess catalytic activities such as oxidase, peroxygenase, superoxide dismutase, and catalase. On account of the intrinsic enzymatic activity of carbon nanomaterials, they can be combined with other materials or modified and functionalized to enhance enzymatic activity. Ye et al. [23] reported a highly specific N-doped nanozyme with HBF as a porous carbonaceous and nitrogen-containing precursor to prepare N-doped carbon nanozymes named HBF-1-c800 by high temperature pyrolysis with N-doping efficiency up to 5.48%, which is higher than the value of most reported N-doped carbon nanozymes. As a result, they found that the apparent POD activity of HBF-1-c800 shows a three to seven-fold enhancement over traditional carbon nanozymes and a five-fold enhancement over the reported N-doped graphene. Consequently, it has been widely used in environmental monitoring and environmental remediation. Although slightly inferior to metal-based nanozymes in terms of catalytic activity, its catalytic activity has been improved, and some excellent designed carbon-based nanozymes show comparable or even better results than that of natural enzymes.

Metal-based nanozymes are one of the most widely used nanozymes. They have unique optical and electrical properties at the nanoscale as well as excellent catalytic properties [24] and exhibit good activity tunability and high stability. They have been found to exhibit a variety of enzyme-like properties, including oxidase-, peroxidase-, catalase-, and/or superoxide dismutase-like activities [25]. Metallic nanomaterials commonly include Au, Ag, Pt, PD, Rh, Ru, and Ir. For metal-based nanozymes, the catalytic mechanism arises from the adsorption, activation, and electron transfer of the substrate onto the metal surface, in contrast to the mechanisms occurring by changes in the metal valence of the nanomaterial, as in the case of other metal compound-based nanozymes [22]. Studies have

found that the surface state of metal-based nanomaterials is one of the important factors affecting their catalytic activity. Therefore, much attention has been focused on how to optimally control the surface of metal-based nanozymes for high electrical conductivity. It can be classified into monometallic nanozymes, bimetallic nanozymes, and multimetallic nanozymes, which are distinguished, as the name implies, by having several metal cores. Bimetallic nanomaterials (BNMS) usually exhibit stronger catalytic performance than monometallic nanomaterials due to the synergistic effect [26], among which platinum-based BNMS have been extensively studied in the field of catalysis for many years. Multimetallic NPs composed of at least three different metals have more possibilities in modulating the activity, selectivity, and stability of surface catalyzed reactions. Hence, the rational design and controllable synthesis of multimetal nanozymes are of great significance.

Transition metals other than noble metals (Ti, V, Cr, Mn, Fe, Co, Ni, Zn, Al, Mo, and W) usually exist stably in the form of their complex ions, among them the oxide form, thus constituting metal oxide-based nanozymes. Metal oxide-based nanozymes including CeO_2, Fe_2O_3, Fe_3O_4, Co_3O_4, Mn_2O_3, and Mn_3O_4 all exhibit multienzyme activities, such as peroxidases, oxidases, hydrolases, and catalases. In addition, they show other physicochemical properties such as fluorescence quenching, dielectric properties, and magnetism [27]. It is worth noting that most metal oxide nanomaterials exhibit lower Km than HRP, which provides the possibility for a wide range of applications. Metal-organic frameworks (MOFs) are porous coordination crystalline materials formed by the self-assembly of metal ions (or metal clusters) and organic ligands through the principles of coordination chemistry [28]. In recent years, some MOFs exhibit their own good enzyme mimicking properties, mimicking the functions of a variety of enzymes, including oxidases, peroxidases, catalases, superoxide dismutases, and hydrolases. The high specific surface area, homogeneously dispersed active sites, structural diversity, and pore size tunability of MOFs can facilitate the efficient contact of reaction substrates to the catalytic sites and, in turn, enhance the catalytic efficiency of subsequent processes. Therefore, its pore size, size, modification, and composition are important factors for regulating enzyme activity. In addition, it can also participate in regulation by external conditions pH, temperature, H_2O_2, and so on [29]. The development of other nanomaterials with different structures and properties has provided new sources for artificial enzyme research, such as perovskites, metal sulfides, metal, dichalcogenides, methyl hydroxides, metal phosphates, and polymeric nanostructures [22]. The development of other types of nanomaterials has provided new sources for artificial enzyme research, such as perovskites, metal sulfides, metal, dichalcogenides, methyl hydroxides, metal phosphates, polymeric nanostructures, and others. They can also mimic the enzymatic activity properties of the oxidoreductase family and have received much attention for their unique structures or properties that are different from those of carbon-based nanomaterials, metal-based nanomaterials, and metal oxide nanomaterials and applications in environmental monitoring and remediation. As a carbon nitride, MXENEs have large surface areas, metallic conductivity, antimicrobial activity, and biocompatibility [30] and have been found to possess intrinsic peroxidase-like and oxidase-like activities and can be enhanced by single stranded DNA (ssDNA) adsorbed onto nanosheets. Li et al. constructed a simple label-free colorimetric sensing platform for TB-selective detection based on Ti_3C_2@ssDNA. The sensor exhibited good selectivity and sensitivity with a wide linear range of 1.0×10^{-11} to 1.0×10^{-8} m and a low detection limit of 1.0×10^{-11} M [31].

In this review, we summarize the most recent applications of nanozymes for environmental monitoring, environmental management, and environmental protection (Figure 1). We firstly introduce the tuning catalytic activity of nanozymes according to some crucial factors such as size and shape, composition and doping, and surface coating. Then, the application of nanozymes in environmental fields is introduced in detail. Nanozymes can not only be used to detect inorganic ions, molecules, organics and foodborne pathogenic bacteria but are also involved in the degradation of phenolic compounds, dyes, and antibiotics. The capability of nanozymes was also reported for assisting air purification, constructing biofuel cells, and application in marine antibacterial fouling removal. Finally,

the current challenges and future trends of nanozymes toward environmental fields is proposed and discussed.

2. Tuning Catalytic Activity

Nanozymes are alternatives to natural enzymes but remain slightly inferior in catalytic activity. Thus, we need to focus on several important factors that affect the enzymatic activity of nanozymes as well as current strategies to enhance activity, thereby laying a theoretical foundation for the design of nanozymes.

One of the distinct features of enzymes are their ultrahigh reaction rate. Correspondingly, nanozymes with comparable or even superior activity are long-standing pursuits. Two strategies are discussed here to improve the activity of nanozymes: (I) increasing the inherent activity by delicate design and (II) boosting the activity by confinement effect or external stimulators [32]. The main factors affecting the intrinsic activity of nanozyme are size, composition, doping, shape, and surface modification. External stimulus factors, such as pH, substrate concentration, temperature, and light, affect the catalytic activity. Factors determining the activity of nanozymes need to be optimized for specific conditions in order to achieve maximum efficiency in applications involving detection of target analytes.

2.1. Size and Shape

Size, shape, and atomic arrangement can lead to changes in the catalytic performance of materials. It was found that the catalytic activity and stability of nanozyme increased with the increase in surface volume ratio. For example, Valden et al. [33] prepared gold clusters with a diameter of 1 to 6 nm on the single crystal surface of titanium dioxide under ultrahigh vacuum to investigate the size dependence of their low-temperature catalytic oxidation of carbon monoxide. It was found that the gold cluster with the largest carbon monoxide oxidation activity was 3 nm. In another case, Zhou et al. [34] used Au nanoparticles with various sizes (2–15 nm) to catalyze the reduction of resazurin, showing that Au nanoparticles of 6 nm exhibited the highest activity. However, small gold nanoparticles tend to aggregate and lose their activity. Scientists often anchor gold nanoparticles to carbon, silica, graphene, and other supporting materials to improve the dispersion of bare Au. Kalantari et al. [35] adjusted the delayed addition time of the thiolated organosilica precursor to control the nanostructure and the thiol density. Moreover, for the first time, they demonstrated that the peroxidase-like activity of T-Dendritic Mesoporous Silica Microspheres (DMSNs)-Au depended on nano-Au size. In addition, the highest activity was achieved at the Au particle size of 1.9 nm (Figure 2).

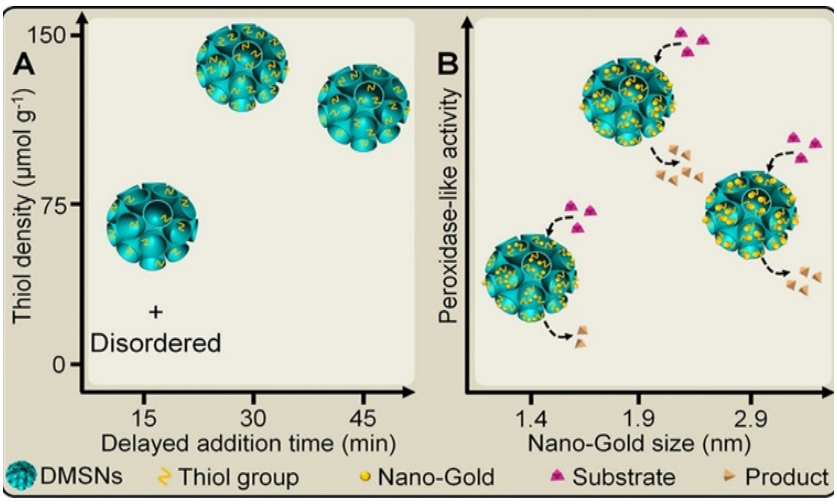

Figure 2. Schematic illustration of the effects of (**A**) delayed addition time on the structures of the final product and (**B**) Nano-Au size on the peroxidase-like activity [35]. Reproduced with permission from Ref. [35], Copyright 2019 American Chemical Society.

The catalytic performance of nanozymes can also be modulated by adjusting the shape of the nanostructures. Biswas et al. [36] compared the catalytic efficiency of gold nanorods (GNRs), gold nanoparticles (GNPs), and horseradish peroxidase (HRP). It was proved that the peroxidase activity of gold nanorods with a length diameter ratio of 2.8 was 2.5 times higher than that of HRP and gold nanoparticles, which showed stability in a wide range of pH and temperature. Based on this, a colorimetric sensor for malathion was developed, whose sensitivity of the assay was 1.78 μg/mL. A comparative study of VO_2 nanoparticles with different morphologies (nanofibers, nanosheets, and nanorods) was conducted and applied to the sensitive colorimetric detection of H_2O_2 and glucose by Tian et al. [37]. According to the typical Michaelis–Menten curve obtained for VO_2 nanozymes, the apparent K_M values of VO_2 nanofibers with H_2O_2 as the substrate were lower than that of VO_2 nanorods and VO_2 nanosheets. It shows that the VO_2 nanofibers have a higher affinity for H_2O_2 compared with VO_2 nanosheets and VO_2 nanorods. Moreover, compared with VO_2 nanorods and VO_2 nanosheets, the VO_2 nanofibers demonstrated the most sensitive response during the H_2O_2 and glucose sensing.

2.2. Composition and Doping

Some researchers have shown, based on the synergistic effect, that combining a variety of nanomaterials or conjugating several nanomaterials to form a hybrid can provide a catalytic center [38], improve the electron transfer between the nanozyme and the substrate, and generate additional active sites, which can adjust the catalytic activity of the catalyst.

Zhu et al. [39] combined TiO_2, $CuInS_2$, and CuS into a ternary metal sulfide-based hybrid. Owing to the synergistic effect among TiO_2, $CuInS_2$, and CuS components, compared with the control sample of Fe_3O_4/rGO, TiO_2/rGO, Fe_3O_4, TiO_2, and rGO, the prepared TiO_2/$CuInS_2$/CuS nanofibers showed excellent peroxidase (POD)-like activity. They subsequently developed a sensor for the detection of dopamine with a detection limit of 1.2 μM. Wang et al. [40] incorporated iron oxide nanoparticles (Fe_3O_4NPs) into the heterodimer composed of gold and platinum to form a hybrid nanomaterial with good peroxidase-like activity. The formation of an alloy between platinum and gold can significantly improve the activity and selectivity of platinum-based catalysts. The nature of the peroxidase-like activity of the Fe_3O_4@Au-Pt hybrid nanomaterial originates from their ability to transfer electrons between the reducing substances and H_2O_2. The colorimetric sensor with a lower detection limit of 0.0018 μM was developed for glucose. Another form of composition is loading. Zhao et al. [41] covalently fixed the carbon point (C-dots) on the inner surface of the amino terminated dendritic silica sphere (dSs) while coupling the gold nanoclusters (Au NCs) on the outer surface. It not only maintains the superoxide dismutase-like enzyme activity of the carbon point but also improves the peroxidase-like-activity of the gold nanoparticles. Furthermore, adjusting the loading ratio of the two kinds of nanozymes can meet different functional requirements.

2.3. Surface Coating

The surface modification of nanozyme not only plays a connecting role in the combination of nanomaterials but also is of great importance to the regulation of catalytic activity. The surface catalytic reaction process can be described by several basic reaction steps, including substrate adsorption, substrate diffusion on the surface, chemical reaction, and then product desorption to regenerate the active site [42]. Each step will be affected by surface modification. Thus, some general strategies can be adopted for surface modification, such as changing the electronic structure of the surface, regulating the surface acidity, blocking surface contact, promoting product desorption, mediating the exposure of active sites to regulate substrate binding, and applying effective methods for surface electronic structure.

Surface modifiers can be divided into three categories: ions, small molecules, and macromolecules. Lee et al. [43] introduced $Mn(acetate)_2$ during the synthetic step of N-doped carbon dots to improve the enzymatic properties of metal-induced N-doped carbon dots (N-CDs). Its influence on the enzymatic properties of Mn-induced N-CDs (Mn:N-CDs)

was investigated. Finally, the addition of Mn(acetate)$_2$ to the reaction solution seemed to generate more functional groups at the edge of carbogenic domains in Mn:N-CDs than in N-CDs, resulting in improved peroxidase-like properties (Figure 3a). Mn:N-CDs with strong enzymatic effects can be applied as a colorimetric sensor probe for the detection of gamma-aminobutyric acid (GABA). Surface modification can also change the intrinsic enzyme activity of nanomaterials. Zeolitic imidazolate framework-8 (ZIF-8) is a monatomic nanozyme with peroxidase activity. Sun et al. [44] introduced amino acid (AA) to regulate the growth of ZIF-8 crystal, thus simulating the structure and function of natural carbonic anhydrase (CA). Amino acid as a capping agent regulates the shape and size of ZIF-8 and forms a hydrophobic region on the surface of ZIF-8 to simulate the hydrophobic pocket of natural carbonic anhydrase (Figure 3b). Compared with natural carbonic anhydrase, Val-ZIF-8 not only has excellent esterase activity but also has better hydrothermal stability. Surface coating may also weaken or even lead to loss of enzyme activity. Jain et al. [45] reported the replacement of cetyl trimithyl ammonium bromide (CTAB) by 11-MUA from the surface of Au-core CeO_2-shell NP-based nanozyme studied for exhibiting multiple enzyme-like activities such as peroxidase, catalase, and superoxide dismutase. They found that 11-MUA coating AuNPs lost the SOD and catalase-like activity, which compromise the multifunctional property of chitosan nanoparticles (CSNPs).

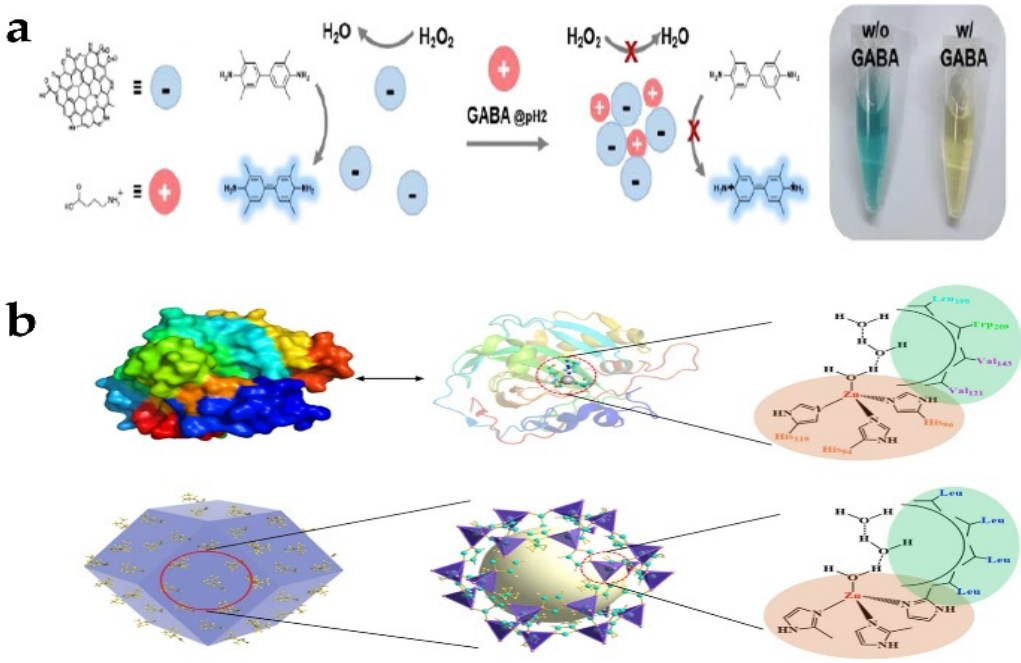

Figure 3. (**a**) Schematic of the peroxidase mimetic activity of Mn:N-CDs [43]. (**b**) Molecular structures of carbonic anhydrase II (CAII) and its active center as well as schematic illustration of the ZIF-8 structure and its CA-mimetic active center [44]. Reproduced with permission from (**a**) Ref. [43], Copyright 2021 Multidisciplinary Digital Publishing Institute; (**b**) Ref. [44], Copyright 2022 American Chemical Society.

2.4. Other Factors

Except regulating the intrinsic enzyme activity of nanozyme to control catalytic activity, external factors can also affect the final enzyme activity. The pH and temperature are the main external influencing factors. A lot of studies have confirmed that acidic conditions are suitable for peroxidase-like activity, while neutral and alkaline conditions are favorable for superoxide dismutase and catalase. For example, the esterase activity of Val-ZIF-8 synthesized by Sun et al. [44] would greatly increase with the increase in temperature. The enzyme activity at 80 °C was about 25 times higher than that at 25 °C. Gao et al. [46] reported a new strategy for controlling plaque biofilm with a peroxidase-like nanozyme (CAT-NP).

CAT-NP showed a strong dependence on acidic conditions. It killed 99% of bacteria in the acidic microenvironment simultaneously in a short time for biofilm control and prevention of dental caries. However, several studies have broken through the limitation of optimal pH for different nanozymes. Li et al. [47] developed the copper-based nanozyme ($CuCo_2S_4$), which showed enhanced peroxidase-like activity and antibacterial ability under neutral conditions (Figure 4). This would be used for infected wounds with pH close to neutral.

3. Improvement of the Specificity

At present, the research of nanozyme is not only to improve catalytic activity but also to improve specific recognition ability to realize the replacement of natural enzyme. The activity change of nanozyme is related to the action mechanism of nanozyme, while the catalytic specificity of nanozyme affects the accuracy of target capture. Most applications of nanozymes are based on the discovery and simulation of nanozyme activity, but there is still a lack of catalytic specificity. The simulation of catalytic activity mostly comes from the functional replica rather than the remodeling of the active center structure of natural enzyme, so the catalytic specificity is greatly reduced. In the years of rapid development of nanozyme, some strategies have been explored to solve these problems: (I) to simulate the active center and binding site of natural enzyme more precisely from the chemical structure at the design and construction of nanozyme and (II) to combine some specific molecular-assisted recognition.

The premise for natural enzyme to work is to combine it with the substrate, that is, to capture the substrate. It mostly depends on the primary structure and spatial configuration of protein or RNA to realize the complementarity with specific substrate. Therefore, the research on the specificity of nanozyme can start from this point. Currently, there have been many reports on biomimetic research of nanozyme [48–50]. For example, Zhou et al. [48] proposed a chiral COF nanozyme with highly ordered active centers and substrate binding sites that is mainly used to simulate horseradish peroxidase (HRP). The active site of HRP contains porphyrin heme as the catalytic active center and the distal L-histidine (L-His) residue as the binding site. Biomimetic COF enzyme is mainly constructed by mixing iron 5, 10, 15, 20-tetra (4′-tetraphenylamino) porphyrin unit (Fe-ATPP) into the COF skeleton as the active center and modifying L-His as the substrate binding site for chiral recognition. COF can be used as the skeleton of nanozyme. The well-dispersed Fe-ATPP unit in the skeleton endows COF nanozyme with high enzyme-like activity, which is 21.7 times higher than HRP. At the same time, the incorporation of L-/D-Hiss imparts the COF nanozyme with enantioselectivity in the oxidation of L-/D-dopa enantiomers and displays a preference for dopa. Changing the content of L-/D-Hiss can also optimize the selectivity of COF nanozyme. This work can easily adjust the activity and stereospecificity of COF chiral nanozyme by changing the doped amino acid and its content.

Although the biomimetic simulation of active centers and binding sites can be carried out according to the analysis of the three-dimensional structure of natural enzymes, the biological affinity and structural simulation of nanomaterials are still limited, which still need to be assisted by biological molecules with specific recognition ability. In this method, the biological recognition element and nanozyme are coupled to achieve the dual improvement of catalytic activity and specificity. Biorecognition elements mainly include antibody, DNA, aptamer, molecularly imprinted polymer (MIP), and biological enzyme. Molecularly imprinted polymer (MIP) is a polymer processed by molecular imprinting technology, which leaves a cavity in the polymer matrix and has affinity for selected "template" molecules [51]. Molecular recognition sites of specific target molecules are created in MIP to obtain solid materials with high selectivity for specific target molecules. Zhang et al. [52] initiated polymerization on the surface of the nanozyme substrate conjugate by adding a variety of polymerization monomers, thus forming a molecular imprinted hydrogel layer. Remove the imprinted substrate molecule to obtain the substrate specific recognition site constructed on the periphery of the nanozyme (Figure 4a). In addition, the incorporation of functional monomers and charges further improved the activity and specificity of

nanozyme. Under the optimum conditions, the specificity can reach 100 times. A variety of nanozyme materials, including ferric oxide, gold, cerium dioxide, and other nanomaterials with peroxidase or oxidase activity, can be significantly improved by molecular imprinting.

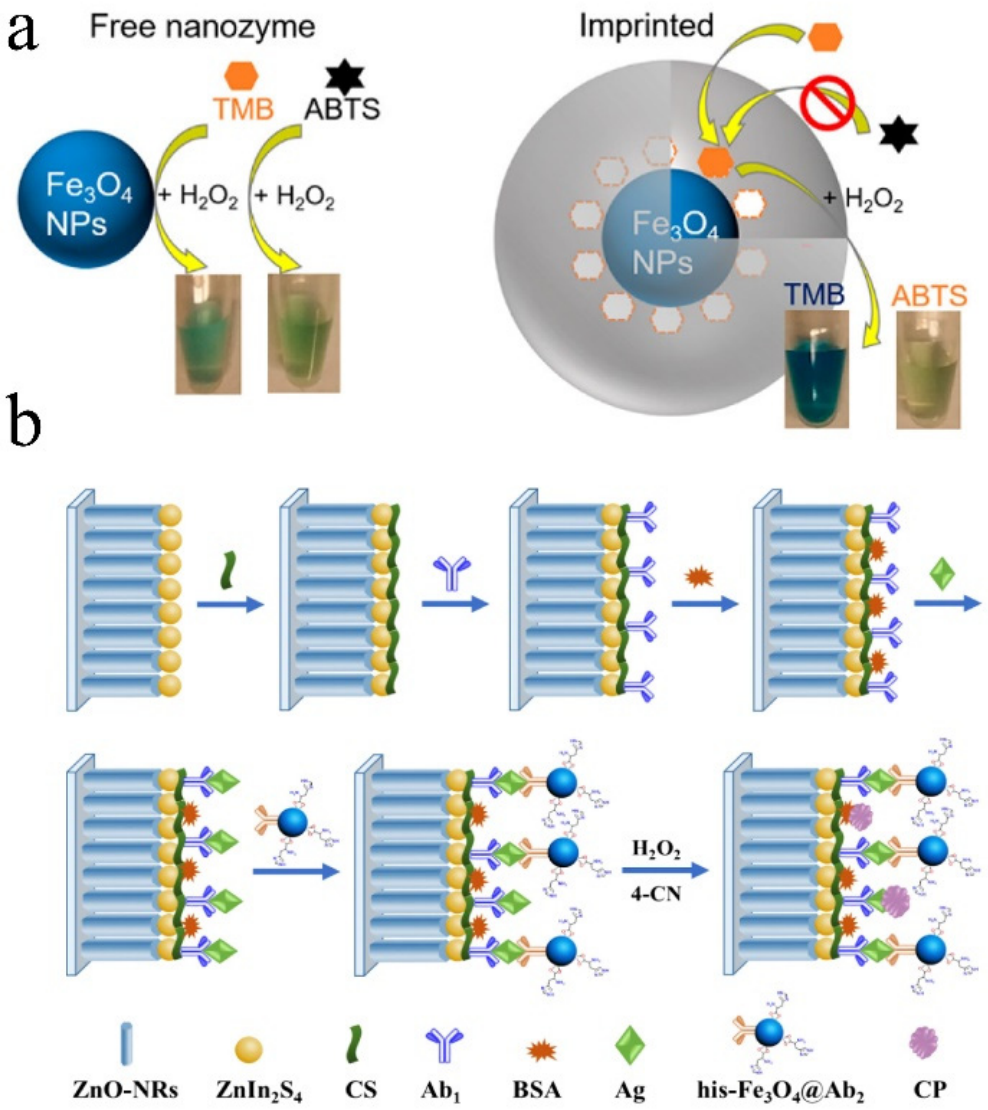

Figure 4. (**a**) Schematic diagram of molecularly imprinted nanozyme preparation [52]. (**b**) Schematic diagram of the PEC immunoassay using high-activity Fe_3O_4 nanozyme as signal amplifier. Reproduced with permission from (**a**) Ref. [52], Copyright 2017 American Chemical Society; (**b**) Ref. [53], Copyright 2019 Elsevier.

The biological enzyme–nanozyme cascade sensing system combined with biological enzyme is mostly used in the application of peroxide–nanozyme. Biological enzymes combine to oxidize specific substrates and produce H_2O_2, which in turn triggers peroxide nanozyme color or fluorescence reaction to realize signal sensing. Although biological enzymes can selectively capture target molecules, just like the reason for the birth of nanozymes, biological enzymes are limited by pH, temperature, reaction system, and other factors. At present, two kinds of enzymes are often linked on the same carrier for a cascade reaction. The ratio of enzyme content, immobilization method, and intermediate loss all affect the catalytic efficiency and sensing accuracy. The highly variable region of the antibody endows the antibody with the ability to recognize antigen specifically. Researchers often use nanozyme to replace the biological enzyme in ELISA to provide color signals. In addition to recording optical (colorimetric, fluorescent, chemilumines-

cence) signals for analysis, nanozyme catalysis can also trigger changes in temperature, volume, mass and pressure to form a new sensing mode. The detection methods are not confined to colorimetric detection but can also use electrochemical detection and Raman analysis. Li et al. [53] used high-activity Fe_3O_4 nanozyme as a signal amplifier to develop an ultrasensitive photoelectronic (PEC) immunoassay. In short, ZnO nanorods (ZnO-NRs) growing vertically on a bar indium–tin oxide (ITO) electrode were dispersed with $ZnIn_2S_4$ nanocrystals, producing a $ZnIn_2S_4$/ZnO-NRs/ITO photoelectronic as the PEC material mix to modify and capture PSA antibodies (Ab_1). Histidine-modified Fe_3O_4 (His-Fe_3O_4) nanozyme acts as a signal amplifier and connects with the signal PSA antibody (Ab_2) to form His-Fe_3O_4@Ab_2 conjugate, which is anchored by a specific sandwich immune reaction (Figure 4b). Labeled His-Fe_3O_4 nanozyme as a peroxidase induced the production of insoluble and insulating precipitation, resulting in a significant reduction of photocurrent signal. Finally, the ultralow detection limit of prostate specific antigen (PSA) 18 fg/mL was achieved. Recently, the methods that can be used for the biological coupling of nanozyme and an antibody are still limited. The technology that can effectively biocouple nanozyme with an antibody or antigen is not mature [19], and the reproducibility of nanozyme-labeled immunosensor is not good, and the large-scale commercial application technology still needs to be developed.

Deoxyribonucleic acid (DNA) and aptamers are other biological recognition elements that assist nanozymes to achieve high specificity. DNA, which follows the principle of complementary base pairing and has a specific sequence, can accurately identify the target, which is widely used in biological and medical fields. However, there are some problems to be solved in the nanozyme labeled with single-stranded DNA (ssDNA). ssDNA endows the surface of nanozyme with more negative charges, which will further affect the adsorption kinetics of substrate and the catalytic activity of nanozyme. It has been found that the modification of DNA changes the surface charge state of Fe_3O_4NPs, thus promoting the combination of nanozyme and substrate [54]. In addition, chemical modification or physical adsorption of DNA may also block the active site of nanozyme, resulting in the reduction of catalytic efficiency. Therefore, the length, concentration, and two-dimensional structure of DNA and the surface charge distribution of nanozyme affect the catalytic activity of nanozyme [55]. Although there have been many research outputs of DNA-modified nanozymes, we still do not know enough about the mechanism of the interaction between the DNA chain on the surface of the nanozyme and the nanozyme. Most of the results are due to the trial and error of scientific researchers. Understanding the mechanism may better control the application of DNA in the field of nanozymes. The aptamer is a short DNA sequence screened in vitro, which is also highly specific. There are many aptamer sensors based on nanozyme. A simple and low-cost colorimetric analysis was established for a highly sensitive determination of Kanamycin (KAN) through integrating boron nitrate quantum dots-anchored porous CeO_2 nanorods (BNQDs/CeO_2) and aptamer by Zhu et al. [56] due to the large specific surface area and synergistic interaction between BNQDs and CeO_3, which can effectively catalyze the oxidation of 3,5′,5,2′-tetramethylbenzidine (TMB). In addition, the catalytic activity of BNQDs/CeO_2 nanozyme was significantly enhanced because of the dispersion of BNQDs/CeO_2 nanozyme and the increase in substrate affinity after the substrate was combined with KAN-specific aptamer. KAN can combine with the aptamer to reduce the catalytic efficiency. The proposed colorimetric method realized the low detection limit of 4.6 pM. DNA and aptamer are superior to other biological recognition molecules in cost and stability, and aptamer can also further improve the detection specificity. However, there is also a complex interaction between the aptamer and the catalytic performance of nanozyme. Mechanism analysis and rule summary need to be obtained.

4. Environmental Monitoring

Over recent years, with the development of industry, environmental pollution has become increasingly serious, especially water pollution, which directly threatens human

health. Common pollutants include heavy metal ions, dyes, phenols, pesticides, antibiotics, drugs, plasticizers, and other organic substances due to biological pollutants such as biological pathogenic bacteria or toxin pollution (Table 1). Hence, monitoring environmental pollutants has become a global concern.

4.1. Toxic Ions

With the rapid development of manufacturing industry around the world, overexploitation of minerals and groundwater, and industrial wastewater discharge, toxic ion pollution has become an unavoidable environmental problem. Toxic ions mainly refer to heavy metal ions, including mercury, cadmium, lead, chromium, arsenic, and other elements with potential biological toxicity. Because it cannot be degraded, it can only be converted into different chemicals through abiotic or biological mechanisms and can be amplified through the food chain, posing a serious threat to the ecosystem and human health [57]. At present, many methods based on nanozyme detection of toxic ions have been explored. Most of the sensors are miniaturized and portable to be used in point-of-care testing (POCT).

Wang et al. [58] loaded Au NPs onto HS-rGO to modify a glass carbon electrode (GCE) as a sensing platform. Au Pd-modified zirconium metal organic skeleton (AuPd@UiO-67) labeled with signal chain (Apt2) is used as signal enhancer to capture Hg^{2+} based on T-Hg (II)-T structure (Figure 5a). With the increase in modified Hg^{2+} concentration, the amount of Apt2-AuPd@UiO-67 is increased, thus realizing the detection of Hg^{2+}. The electrochemical sensor has a wide linear range (1.0 nmol/L–1.0 mmol/L) and a low detection limit (0.16 nmol/L). Except for electrochemical detection methods, colorimetry is the most commonly used method to detect Hg^{2+}. A graphene oxide nanosheet (CGO) based on L-cysteine functionalization was found to have a strong peroxidase-like activity compared with graphene oxide [59]. The introduction of more S and N species can effectively produce more surface defects and active sites, thus endowing carbon high peroxidase-like properties. The nanozyme can be used to realize the microdetection of Hg^{2+}, and its sensing principle is mainly based on the competitive adsorption between Hg^{2+} and photothermal properties of 3,3′,5,5′-tetramethylbenzidine (TMB). Because Hg^{2+} hinders the combination of TMB and CGO, TMB is catalyzed by H_2O_2 to produce more colored oxidation products, resulting in a more significant colorimetric response (Figure 5b), meaning, therefore, good detection of Hg^{2+}. Zhong et al. [60] used the peroxidase-like activity of iron hydroxide (FeOOH) nanorods to detect As(V) by colorimetry. Unlike TMB, the catalytic substrate is ABST, and its oxidation product is green and reaches the maximum absorption peak at 418 nm. As(V) can be adsorbed onto FeOOH nanorods through electrostatic interaction and an As-O bond, so the oxidation is gradually embedded. Finally, the colorimetric determination with response of 0–8 ppb and 8–200 ppb and detection limit of 0.1 ppb is realized. Ag^+ is also a heavy metal ion. Zhang et al. [61] utilized the excellent colorimetric and TMB to construct photothermal and colorimetric double-readout sensors for Ag+ analysis. MnO_2 nanosheets (NSs) were used to catalyze the oxidation of TMB to oxTMB. However, the reduction of MnO_2 NSs by glutathione (GSH) can reduce the catalytic capacity of MnO_2 NSs (Figure 5c). In this method, a specific combination of Ag^+ and GSH is utilized to inhibit this reduction process. According to this principle, the Ag^+ concentration can be converted into temperature and color signals. Consequently, the Ag^+ content can be determined both with the naked eye and with a portable thermometer. It is very suitable for POCT in the process of environmental detection.

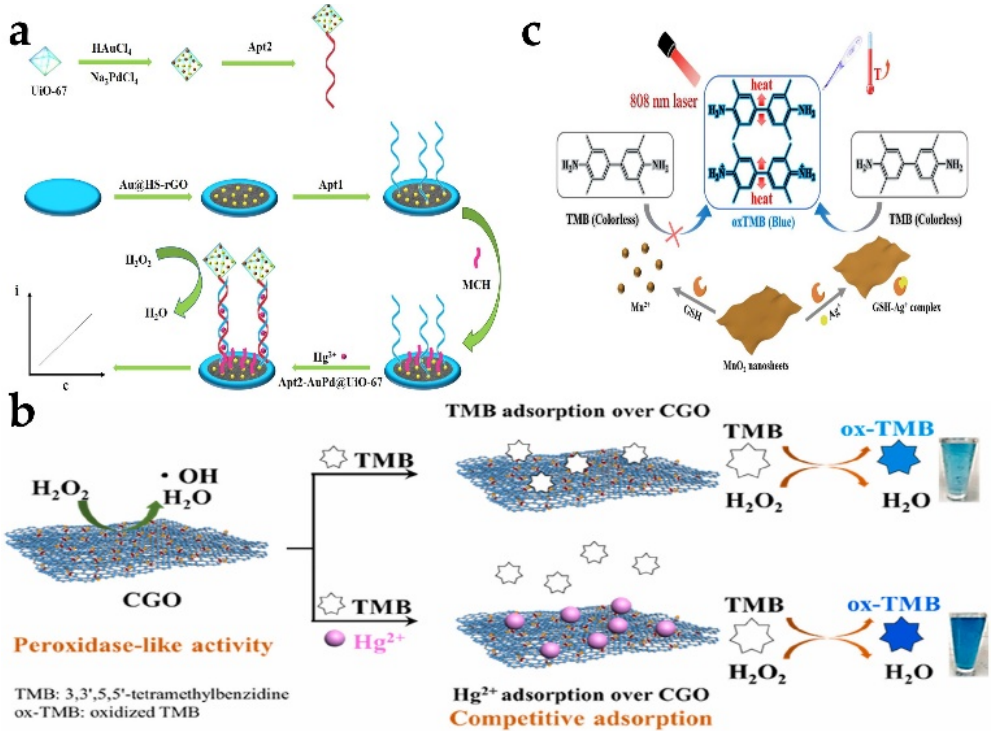

Figure 5. (**a**) Schematic diagram for fabricating the designed electrochemical aptasensor to detect Hg^+ [58]. (**b**) Schematic of CGO preparation and the principle of color rendering [59]. (**c**) Schematic of the proposed MnO_2 NSs-GSH-TMB colorimetric and photothermal platform for the Ag^+ analysis [61]. Reproduced with permission from (**a**) Ref. [58], Copyright 2022 Elsevier; (**b**) Ref. [59], Copyright 2022 Elsevier; (**c**) Ref. [61], Copyright 2019 Springer.

4.2. Organic Pollutants

Herbicides and pesticides used in agriculture to increase food production will cause serious pollution of soil and water quality. At present, most pesticides on the market are not degradable organophosphorus pesticides. If the metabolites or degradation products of pesticides exceed the maximum residue, they will cause pollution. In addition, antibiotic residues are also considered as typical organic pollution. Because of their longer half-life, they are more threatening to humans and other organisms. Another common organic pollutant, phenolic compounds, are common in dye, pharmaceutical, photo development and other industrial fields and is difficult to degrade in the aquatic ecological environment.

Parathion is an organophosphate (OP) insecticide, and it is also an irreversible inhibitor of nervous system function. Chen et al. [62] designed a bimetallic nanozyme (Au@Pt: gold@platinum) catalytic competitive sensitive biological bar code immunoassay. This novel biobarcode immunoassay contained three types of probes: (I) mAbs and ssDNA-labeled AuNP probes, (II) parathion OVA-hapten-modified immunomagnetic nanoparticle (MNP) probes, and (III) C-ssDNA-labeled Au@Pt probes (Figure 6a). The Au@Pt probe reacts with the AuNP probe through complementary base pairing. Parathion then competes with the MNP probe to bind mAb onto the AuNP probe. Finally, Au@Pt nanozyme is released from the complex to catalyze the color development of TMB. The most common and efficient platform to detect OPs is the enzyme biosensor, which is based on OP_S to inhibit acetylcholinesterase (AChE) activity. In another work, lactate dehydrogenase (LDH)-based ZIF-8 nanocomposite was prepared by Bagheria et al. [63], utilizing the formation of a simple complex between Zn^{2+} and 2-methylimidazole. This process leads to the formation of highly dispersed ZIF-8 nanostructures on the surface of ZnFe-LDH nanosheets (LDH@ZIF-8). Moreover, the peroxidase-mimicking behavior of the prepared nanocomposites is improved compared to pristine LDHs and MOFs. LDH@ZIF-8 significantly contributes to the CL emission intensity of the H_2O_2 rhodamine B (RhoB) system.

When organophosphorus pesticides (OP_S) were present, AChE activity was inhibited, and reduced production of H_2O_2 eventually led to the attenuated chemiluminescence of RhoB (Figure 6c). This detection method achieved highly sensitive sensing of OP_S indirectly by detecting the change of the hydrogen peroxide content. Apart from the chemiluminescence strategy, photoelectrochemical biosensors are another emerging analytical method. Song et al. [64] used the double amplification strategy to construct the photoelectrochemical aptamer sensor. The sensor realizes signal sensing mainly based on Co_9S_8@In-CdS NTs and PtNi nanozymes acting as signal amplifiers. Because sulfamethazine (SMZ) has a stronger affinity with the aptamer, the aptamer tends to combine with SMZ and escape from the electrode through the dissociation of the double chain structure, generating a photocurrent response. SA-modified PtNi nanostructures further increase the spatial steric resistance of the electrode surface. The insoluble 4-CD precipitate formed by incubation with 4-CN in the presence of H_2O_2 seriously hinders electron transfer and again changes the photocurrent response to achieve sensing of SMZ (Figure 6b).

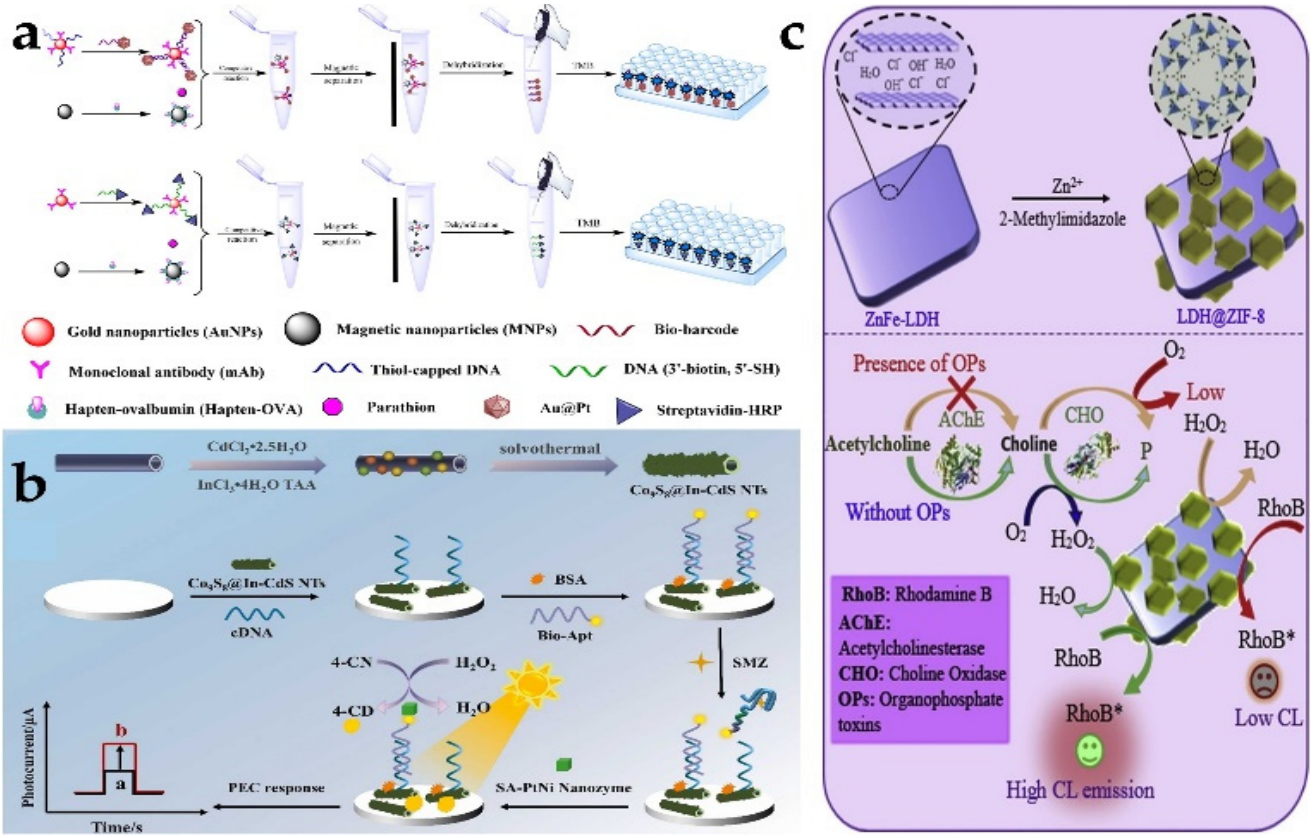

Figure 6. (**a**) Schematic presentation of the colorimetric biobarcode immunoassays for parathion based on amplification using Au@Pt and HRP [62]. (**b**) Schematic illustration of the preparation process of Co9S8@In-CdS NTs and the proposed PEC aptasensor for SMZ detection [64]. (**c**) Detection of OPs by LDH@ZIF-8-assisted RhoB-H_2O_2 CL-based system [63]. Reproduced with permission from (**a**) Ref. [62], Copyright 2020 American Chemical Society; (**b**) Ref. [64] Copyright 2022 Elsevier; (**c**) Ref. [63], Copyright 2019 Elsevier.

In order to make detection and environmental assessment portable and fast, some researchers bind sensors and smartphones to achieve mobile data transmission. This kind of combination can be used for POCT. Sun et al. [65] synthesized a three-layer FeOx@ZnMnFeOy @Fe Mn bimetallic organism with excellent multienzyme activity (peroxidase, oxidase, and catalase). Therefore, this sensing platform can complete the four functions of detecting H_2O_2, citric acid (CA), norfloxacin (NOR), and gallic acid. Moreover, smartphones are also used for automatic quantitative detection of CA and NOR, and the

detection limit of norfloxacin is as low as 52 nM. Nanozyme with multienzyme activity was also used in the detection of phenolic compounds. A highly efficient mimic catalyst of $Co_{1.5}Mn_{1.5}O_4$ with four enzyme activities (peroxidase, oxidase, catalase, laccase) was used to detect dihydroxybenzene isomers. Finally, a dual function colorimetric sensor was constructed using TMB [66]. Ye et al. [67] constructed $NiCo_2O_4$@MnO_2 with p–n junctions, which not only has the photoelectric effect brought by the p–n junctions but also has inherent oxidase and peroxidase-like activities. The result is an excellent minimum detection limit of 0.0042 μM for hydroquinone.

4.3. Foodborne Pathogens

Biological pollution mainly refers to environmental pollution caused by various organisms that pose a threat to human health. The biological pollution in the water and soil environment mainly comes from untreated domestic sewage, industrial wastewater, garbage, and feces, which eventually leads to the excessive content of foodborne pathogens. In history, Vibrio cholerae once polluted the water environment as a foodborne pathogen, which eventually led to the global epidemic of cholera in the 1930s. Intestinal bacteria such as Escherichia coli, Streptococcus faecalis and Clostridium are the main bacteria that pollute water. Hepatitis also erupts through fecal sewage.

The first microorganism to be detected in drinking water is the content of Escherichia coli (*E. coli*). Thus, the detection of foodborne pathogens is increasingly urgent. In the detection of *E. coli*, β-Galactosidase (β-Gal) is applied. A multicolor colorimetric platform triggered by a designed enzyme nanozyme cascade reaction was designed and prepared [68]. MnO_2 nanoparticles with oxidase-like activity can catalyze the oxidation of TMB. Then TMB^{2+} quickly etched the gold nanorods (Au NRs), and the longitudinal local surface plasmon resonance peak appeared as an obvious blue shift and the polychromatic change of Au NRs. The presence of *E. coli* will hydrolyze p-aminophenyl β-d-galactopyranoside (PAPG) to produce p-aminophenol (PAP) through β-galactose, thereby mediating the reduction of MnO_2 nanosheets, destroying their oxidase-mimicking activity, and affecting the production of TMB^{2+}. Consequently, sensing systems that exhibit different colors can be easily observed for different concentrations of *E. coli*. A colorimetric sensor based on Ps-Pt nanozymes for the detection of Salmonella typhimurium was reported by Jiao et al. [69]. The sensor combines immunosensing and magnetic separation techniques. They covalently bound streptavidin first to Ps-Pt. Then the bacteria were recognized by coupling a biotinylated antibody of *S. typhi* onto PS Pt through the high affinity between streptavidin and biotin. Moreover, the magnetic beads conjugated antibodies were also prepared to facilitate the subsequent bacteria separation test, thus making the detection simple and fast. Similarly, Ps-Pt nanozyme with peroxidase activity has also been used to detect *Staphylococcus aureus* (*S. aureus*) on paper-based analytical equipment with a detection limit of 9.56 ng/mL [70]. Targeting *S. aureus*, Luo et al. [71] constructed a PEC sensor for *S. aureus* with a wide linear range between 10 and 10^8 CFU/mL and a limit of detection (LOD) as low as 3.40 CFU/mL based on "signal off" using the Cu-C_3N_4-TIO_2 heterostructure as the photoactive material and Cu-C_3N_4 peroxidase-like nanozymes as signal amplifiers. During the detection, Cu-C_3N_4 (Cu-C_3N_4@Apt) and benzo-4-chlorohexanedione (4-CD) produced by the oxidation of 4-chloro-1-naphthol (4-CN) in the presence of hydrogen peroxide participated in decreasing the photocurrent signal (Figure 7b). Polyoxometalates (POMS) of different structures have also been noted to possess peroxidase activity, among which $P_2Fe_4W_{18}$ enzyme activity was reported by Zhang et al. [72] Polydopamine (PDA) as an emerging biomimetic adhesive polymer combines with $P_2Fe_4W_{18}$ to enhance enzyme activity (Figure 7a). Ultimately, $Fe_4P_2W_{18}$/PDA achieved the detection of *E. coli* O157:H7 with a detection limit of 4.2×10^2 CFU/mL.

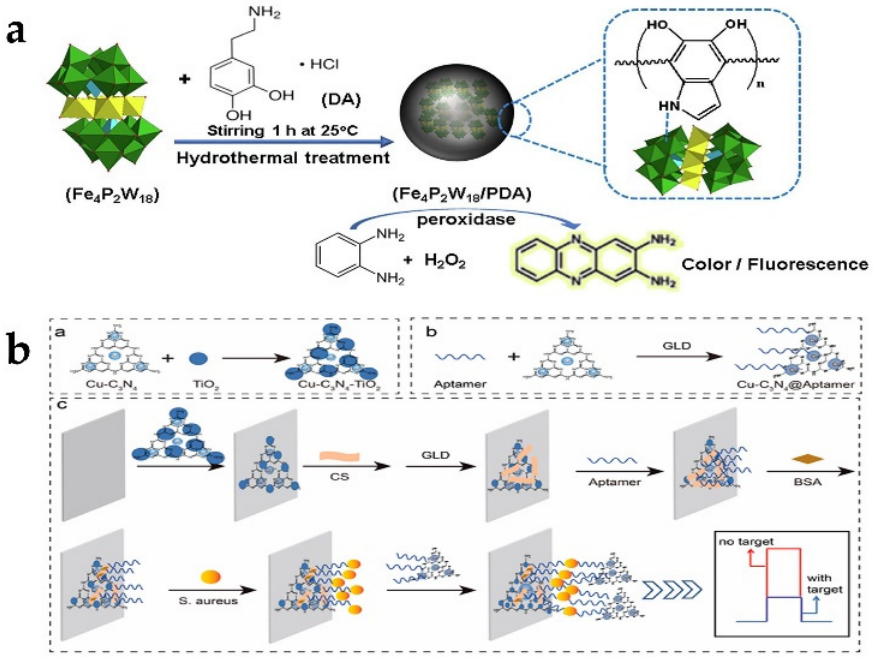

Figure 7. (**a**) Construction of the PEC sensor and detection of S. aureus [72]. (**b**) Schematic illustration of the synthesis procedure and the peroxidase activity of the P2W18Fe4/PDA nanozyme [71]. Reproduced with permission from (**a**) Ref. [72], Copyright 2022 Elsevier; (**b**) Ref. [71], Copyright 2021 Elsevier.

Table 1. Summary of the application of nanozymes in environmental monitoring.

Category	Analyte	Nanozyme	Activity	Detection Mode	Detection Range	LOD	Ref.
Toxic ions	Fe^{2+}/Pb^{2+}	MnO_2	CAT	Colorimetric	0.001~0.02 mmol/L 0.05~0.4 mmol/L	0.5 μmol/L 2 μmol/L	[73]
	F^-	AgPt-Fe_3O_4	POD	Colorimetric	50~2000 μM	13.73 μM	[74]
	Nitrite	AuNP-CeO_2 NP@GO	OXD	Colorimetric	100~5000 μM	4.6 M	[75]
	Cl^-, Br^-, I^-	Ag_3Cit	OXD	Colorimetric	/	26, 12, 7 nM	[76]
	Cu^{2+}	E-ChlCu/ZnO	POD	Colorimetric	0–1/1–15 μM	0.024 μM	[77]
	As^{3+}	Pd-DTT	OXD	Colorimetric	33~3.333 × 10^5 ng/L	35 ng/L	[78]
	Fe^{2+}	C-dots/Mn_3O_4 NCs	OXD	Colorimetric	0.03~0.83 μM	0.03 μM	[79]
	Nitrite	His@AuNCs/RGO	POD	Electrochemical	2.5~5700 μM	0.5 μM	[80]
	Hg^{2+}	MXene/DNA/Pt NCs	POD	Colorimetric	50~250 nM	9.0 nM	[81]
	Fe^{3+}	NCD/UiO-66 NCs	SOD POD	Colorimetric	0~0.1 mM	/	[82]
	Cr^{6+}	PEI-AgNCs	OXD	Colorimetric	/	1.1 μM	[83]
	Fe^{2+}	AuRu aerogels	OXD POD	Colorimetric	5~250 μmol/L	0.7 μmol/L	[84]
	Hg^{2+}	CS-$MoSe_2$NS	POD OXD	Colorimetric	0.1~4.0 μM	3.5 nM	[85]
	Fe^{3+}	$MoSe_2$@Fe	POD	Colorimetric	25~300 μM	1.97 μM	[86]
	F^-	R-$MnCo_2O_4$/Au NTs	POD	SERS	0.1~10 nM	0.1 nM	[87]
	Sn^{2+}	nano-UO_2	POD	Colorimetric	0.5–100 μM	0.36 μM	[88]
	PO_4^{3-}	MB@ZrHCF	POD	Colorimetric	10~200 μM	2.25 μM	[89]
	Cr^{3+}	GdOOH	Phospholipase	Colorimetric	5.0~200 μM	0.84 μM	[90]

Table 1. *Cont.*

Category	Analyte	Nanozyme	Activity	Detection Mode	Detection Range	LOD	Ref.
Toxic ions	Hg^{2+}	AuPd@UiO-67	POD	Electrochemical	1~10^6 mM	0.16 nmol/l	[58]
	Al^{3+}	Single atom Ce-N-C	Laccase	Colorimetric	5–25 μg/mL	22.89 ng/mL	[91]
	Cr^{6+}	CD/g-C_3N_4	POD	Colorimetric	0.3–1.5 μM	0.31 μM	[92]
	Hg^{2+}	CuS HNS	POD	Colorimetric	50~4 × 10^5 ng/mL	50 ng/L	[93]
	As^{3+}	CoOOH	POD	Electrochemical	0.1~200 μg/L	56.1 ng/L	[94]
	Cr^{6+}	Cu-PyC MOF	POD	Colorimetric	0.5–50 μM	0.051 μM	[95]
	Cr^{6+}	Ni/Al LDH (Ni/Al–$Fe(CN)_6$ LDH)	POD	Colorimetric	0.067~10 mM	0.039 mM	[96]
	Pb^{2+}	Tannic Acid@Au NPs	POD	Colorimetric	25~500 ng/mL	11.3 ng/mL	[97]
	S^{2-}	MoS_2/g-C_3N_4HNs	POD	Colorimetric	0.1~10 μM	37 nM	[98]
	S^{2-}	PDA@Co_3O_4NPs	CAT	Colorimetric	4.3~200 μM	4.3 μM	[99]
	As^{3+}	AuNPs	POD	Colorimetric	0.01~11.67 mg/L	0.008 mg/L	[100]
	S^{2-}	GMP-Cu	Laccase	Colorimetric	0~220 μmol/L	0.67 μmol/L	[101]
	Hg^{2+}	Ag_2S@GO	OXD	Colorimetric	5.0~120.0 × 10^{-8} M	9.8 × 10^{-9} mol/L	[102]
	Cu^{2+}	MMoO	POD	Colorimetric	0.1~24 μM	0.024 μM	[103]
	Cr^{6+}	MOF	OXD	Colorimetric	0.1~30 μM	20 nM	[104]
	Cr^{6+}	CuS-frGO	POD	Colorimetric	0–200 nM	26.60 nM	[105]
	Cr^{6+}	SA-Fe/NG	POD	Colorimetric	30~3 μM	3 nM	[106]
	Cr^{3+}	$CuFe_2O_4$/rGO	POD	Colorimetric	0.1~25 μM	35 nM	[107]
	Hg^{2+}	L-cysteine@GO	POD	Colorimetric	0~200 μg/L	5 μg/L	[59]
	Hg^{2+}	PtNPs	POD	Colorimetric	20~3000 nM	10.5 nM	[108]
	Hg^{2+}	Au-HBNz	POD	Colorimetric	0.008~20 μg/mL	1.10 ng/mL	[109]
	Hg^{2+}	AuPt@DSN	POD	Colorimetric	0.1~10^3 nM	8.58 pM	[110]
	Hg^{2+}	MVC-MOF	OXD	Colorimetric	0.05~6 μM	10.5 nM	[111]
	Hg^{2+}	Citrate-capped Cu NPs	POD	Colorimetric	0.100~6.000 μM	0.052 μM	[112]
	Hg^{2+}	Fe-MoS_2@AuNPs	POD	Electrochemical	0.5~200 nM	0.2 nM	[113]
	Hg^{2+}	Ag NWs	OXD	Colorimetric	25~5000 μg/L	19.9 ng/L	[114]
	Hg^{2+}	Cys-Fe_3O_4	POD	Colorimetric	0.02–90 nM	5.9 pM	[115]
	Hg^{2+}	His-AuNCs	OXD	Colorimetric	0.05–0.8 μM	8 nM	[116]
	Ag^{+}	MnO_2 NSs	OXD	Colorimetric	0.02~1.0 μM	6.7 nM	[61]
	As^{5+}	FeOOH	POD	Electrochemical	0.04~200 μg/L	12 ng/L	[60]
	Al^{3+}	Nanoceria	Phosphatase	Electrochemical	30~3.5 × 10^3 nM	10 nM	[117]
	H_2O_2	MA-Hem/Au-Ag	POD	Colorimetric	0.010–2.50 mM	2.5 μM	[118]
	H_2O_2	Pt/CeO_2/NCNFs	CAT	Electrochemical	0.0005–15 mM	0.049 μM	[119]
Phenolic	Phenol Compounds	1-Methylimidazole/Cu Nanozyme	Laccase	Colorimetric	0.5~4 μg/mL	0.57 μg/ml	[120]
	2,4-dinitrophenol	polymer-Fe-doped ceria/Au NC	POD	Colorimetric	1~100 μg/mL	2.4 μM	[121]
	Hydroquinone	$NiCo_2O_4$@MnO_2	POD OXD	Colorimetric	0~24 μM	0.042 μM	[67]
	Hydroquinone	$Co_{1.5}Mn_{1.5}O_4$	OXD	Colorimetric	0.05~100μM	0.04μM	[66]
	2,4,6-TNT	2H–MoS_2/Co_3O_4	OXD	Electrochemical	/	1 pM	[122]
	Hydroqui-none	Fe_3O_4@COF	POD	Colorimetric	0.5~300 μmol L	0.12 μmol L	[123]
	2,4-DP	AMP-Cu	Laccase	Colorimetric	0.1~100 μmol/L	0.033 μmol/L	[124]
	2,4-DP	MnCo@C NCs	Laccase	Electrochemical	3.1~122.7 μM	0.76 μM	[125]
	2,4-DP	$NiFe_2O_4$	POD	Colorimetric	0.218~3.282 μg/mL	0.311 μg/mL	[126]

Table 1. *Cont.*

Category	Analyte	Nanozyme	Activity	Detection Mode	Detection Range	LOD	Ref.
OPs	Carbendazim	MoS_2/MWCNTs	OXD	Electrochemical	0.04~100 μM	7.4 nM	[127]
	parathion ethyl	C-Au NPs	POD	Colorimetric	11.6~92.8 ng/mL	5.8 ng/mL	[128]
	Dichlorvos	γ-MnOOH NWs	OXD	Colorimetric	0~15 ng/mL	3 ng/ml	[129]
	Diazinon	LDH@ZIF-8	POD	Colorimetric	0.5~300 nM	0.22 nM	[63]
	Paraoxon	2D MnO_2	OXD POD	Electrochemical	0.1~20 ng/mL	0.025 ng/mL	[130]
	Benomyl	AgNPs/MWCNTs/GO	OXD	Electrochemical	0.2~122.2 μM	/	[131]
	Dimethoate	Pt NPs	POD	Colorimetric	0.5~9 μg/mL	0.15 μg/mL	[132]
	Naphthalene acetic acid	Ti_3C_2-MXene/BP	OXD	Electrochemical	0.02~40 μM	1.6 nM	[133]
	Parathion	NiO-SPE	OXD	Electrochemical	0.1~30 μM	0.024 μM	[134]
	MeHg	NA-CDs/AuNPs	POD	Colorimetric	0.375~75 μg L	0.06 μg L	[135]
	Chlorpyrifos	Ag-Nanozyme	POD	Colorimetric	35~210 ppm	11.3 ppm	[136]
	Omethoate	SACe-N-C	POD	Colorimetric	100~700 μg/mL	55.83 ng/mL	[137]
	Methyl-paraoxon	Nanoceria	Laccase	Colorimetric	0.42~126 μM	0.42 μmol/L	[138]
	Methyl-paraoxon	CeO_2	POD OXD	Electrochemical	0.1~100 μmol/L	0.06 μmol/L	[139]
	Methyl-parathion	Fe_3O_4/C-dots@Ag-MOFs	/	Electrochemical	5×10^{-11}~2×10^{-9} mol/L	1.16×10^{-11} mol/L	[140]
	Atrazine	Fe_3O_4-TiO_2/rGO	POD	Colorimetric	2~20 mμ g/L	2.98 μg/L	[141]
	Glyphosate	Au@PN	POD	Colorimetric	0.5~20 nM	0.24 nM	[142]
	Glyphosate	Porous Co_3O_4	POD	Colorimetric	8~80 μg/L	2.37 μg/L	[143]
	Glyphosate	Fe_3O_4@C_7/PB	POD	Colorimetric	0.125~15 μg/mL	0.1 μg/mL	[144]
	Carbaryl	NH_2-MIL-101(Fe)	POD	Colorimetric	2~100 ng/mL	1.45 ng/mL	[145]
	Chlorophenols	Fe_3O_4@MnOx	OXD	Colorimetric	10~1600 μM	0.85 μM	[146]
	Fipronil	ZIF-8	POD	Colorimetric	0.2~4μM	0.036 μM	[147]
	Malathion	Fe-N/C SAzyme	OXD	Colorimetric	0.5~10 nM	0.42 nM	[148]
Antibiotic residues	Sulfamethazine	PtNi NCs	POD	Photoelectrochemical	0.05~10^3 pg/mL	37.2 fg/mL	[64]
	Sulfonamides	2D Cu-TCPP (Fe)	POD	Electrochemical	1.186~28.051 ng/mL	0.395 ng/mL	[149]
	Streptomycin	Au@Pt NPs	POD	Lateral Flow Immunoassays	0.062~0.271 ng/mL	1 ng/mL	[150]
	Tetracycline	Cu-doped-g-C_3N_4	POD	Colorimetric	0.1~50 μM	31.51 nM	[151]
	Tetracycline	Fe_3O_4@MIP	POD	Colorimetric	2~225 μM	0.4 μM	[152]
	Tetracycline	MIL-101(Fe/Co)	POD	Colorimetric	1–8 μM	0.24 μM	[153]
	Norfloxacin	FO@ZMFO@FM-MOG	CAT OXD POD	Colorimetric	0.415–6.21 μM	52 nM	[65]
	Kanamycin	$CoFe_2O_4$NPs	POD	Electrochemical	1~10^{-6} μM	0.5 pM	[62]
	Chloramphenicol	Co_3O_4	POD	Electrochemilumi-nescence	5×10^{-13}~4×10^{-10} mol/L	1.18×10^{-13} mol/L	[154]
	Kanamycin	WS_2 Nanosheets	POD	Colorimetric	0.1–0.5 μM	0.06 μM	[155]
	Metronidazole	MIL-53 (Fe)@ molecularly imprinted polymer (MIP)	POD	Colorimetric	1~200 μM	53.4 nM	[156]
Foodborne pathogens	*Staphylococcus aureus*	Cu-C_3N_4-TiO_2	POD	Photoelectrochemical	10~10^8 CFU/mL	3.40 CFU/mL	[71]
	Staphylococcus aureus	Pd@Pt NPs	POD	Lateral Flow Immunoassays	10–300 ng/mL	9.56 ng/mL	[70]
	Salmonella typhimurium	IPs-Pt	POD	Colorimetric	10^4~10^6 CFU/mL	10^3 CFU/mL	[69]
	Escherichia coli	Au NRs	OXD	Colorimetric	1.0×10^2~1.0×10^5 CFU/mL	22 CFU/mL	[68]
	E. coli O157:H7	Au-Pt dumbbell NPs	POD	Colorimetric	10~10^7 CFU/mL	2 CFU/mL	[157]
	E. coli O157:H7	man-Pediatric lead (PB)	POD	Lateral Flow Immunoassays	10^2~10^8 CFU/mL	10^2 CFU/mL	[158]
	E. coli O157:H7	$P_2W_{18}Fe_4$/PDA	POD	Colorimetric	10^3~10^6 CFU/mL	4.2×10^2 CFU/mL	[72]

5. Environmental Management

Over these years, industrial development and natural resource exploitation have brought economic prosperity, but at the same time, all over the world, it has also faced serious environmental governance challenges. Most pollutant residues are found in water sources and soils on which mankind depends for survival. Furthermore, the common degradation methods of pollutants are of three types: (I) biodegradation, (II) physical adsorption, and (III) chemical oxidation. Nanozymes as an emerging research outcome in the 21st century exhibit excellent qualities in environmental governance. They (I) can handle compounds that are often difficult to biodegrade, (II) can operate independently of pollutant concentration, (III) can operate over a wide range of pH, temperature, and salinity, (IV) are not inhibited by biofouling, (V) are relatively simple and easy to control, and (VI) are highly stable and recyclable [57]. Environmental monitoring Table 2 demonstrates the application of nanomaterials in the degradation of various pollutants.

Table 2. Summary of the application of nanozymes in environmental management.

Category	Pollutant	Activity	Nanozyme	Removal Efficiency	Ref.
Dyes	RhB	POD	Sulfur-doped graphdiyne	>98%	[159]
	Methyl orange	POD	CNZ	93%	[160]
	Rhodamine B	OXD	FeBi-NC SAzyme	99%	[161]
	Methylene Blue	POD	ZnNi-MOF/GO NCs	95%	[162]
	Methylene Blue	POD	Cu^{2+}-HCNSs-COOH	80.7%	[163]
	Methylene Blue	POD OXD	PdNPs/PCNF	99.64%	[151]
	Amido Black	Laccase	Cu/H_3BTC MOF	60%	[164]
	Malachite green	Laccase	Fe_3O_4@C-Cu^{2+}	99%	[165]
	Organic dyes	POD	Fe_3O_4@Gel	99%	[166]
Antibiotics	Tetracycline	POD	Sulfur-doped graphdiyne	>69%	[159]
Toxic ions	Cr^{6+}/As^{3+}	CAT	$NanoMn_3O_4$	>98%	[167]
	Hg^{2+}/Cl^{-}	POD	AgRu@β-CD-co-GO	94.9% 93.8%	[168]
	H_2O_2	CAT POD	DMNS@AuPtCo	>95%	[169]
Phenolic	Hydroquinone	Laccase	Aminopropyl-functionalized copper containing phyllosilicate (ACP)	100%	[170]
	Phenol	POD	MNP@CTS	>95%	[171]
	Phenol	CAT POD	DMNS@AuPtCo	90%	[169]
	2,4-DP	Laccase	Fe1@CN-20	65%	[172]
	2,4-DP	Laccase	AMP-Cu	65%	[124]
	2,4-DP	Laccase	CH-Cu	82%	[173]
	2,4-DP	Laccase	Cu-Cys@COF-OMe	>75%	[174]
	2,4-DP	Laccase	CA-Cu NPs	90%	[175]
	DEHP phthalic acid esters	Hydrolase	Zn-heptapeptide bionanozymes	86.80%	[176]
	Microplastics	POD	Fe_3O_4NPs	100%	[177]
Pathogens	*Escherichia coli*	Phospholipase	PAA-Cnp	>80%	[178]
	Escherichia coli	POD	Au-Pt dumbbell NPs	95%	[157]
	Escherichia coli	OXD	w-SiO_2/CuO	90%	[179]
	Gram-negative bacteria	POD	SA-Pt/g-C_3N_4-K	>99.99%	[180]
OPs	Simazine	POD	Fe_3O_4/DG	99%	[181]
	Atrazine	POD	Fe_3O_4-TiO_2/rGO	98%	[141]
	Cinosulfuron	POD	CP@CA	96.25%	[182]

Currently, most of the substances that nanozymes are able to degrade are organic such as phenolic compounds, herbicides, insecticides, dyes, and antibiotics. A few nanozymes are used to degrade inorganic heavy metal ions. Citric acid-modified copper peroxide nanodots (CP@CA) synthesized by Yang et al. [182] are an autocatalytic nanozyme. Under acidic conditions, they can decompose into H_2O_2 and Cu^{2+} in water or soil, while H_2O_2 would further decompose into •OH, capable of degrading nicosulfuron, based on a Fenton-like reaction. Its degradation rate can reach 97.58% within 1 h. Furthermore, after CP@CA was involved in pollutant degradation, the ecotoxicity of most degradation intermediates was reduced to a lower level compared with nicosulfuron. Moreover, CP@CA had little effect on the active components of the soil bacterial community. Photocatalytic degradation is another pathway for the degradation of pollutants. Baruah et al. synthesized magnetic Fe_3O_4 NPs on the surface of polydopamine functionalized RGO sheets (FDGs) for photocatalytic degradation of the hazardous pesticide simazine. Due to its excellent photocatalytic activity and magnetic separability, this makes the degradation rate of this nanozyme 99% and highly sustainable. The specific mechanism of its degradation relies on the formation of •OH under photocatalysis. The graphene sheets with good optical properties enhanced Fe_3O_4 with very high electron hole pair recombination characteristics. Dopamine-functionalized graphene sheets (DG) have high electron carrier capacity through their π-bond network, resulting in FDG nanozymes with high photocatalytic activity. Upon light irradiation, nanozymes absorb photons and undergo redox reactions by elevating electrons from the valence band (VB) to the conduction band (CB) (Eq^n 8). The electrons in the CB can be easily transferred to the DG surface, forming a hole in the VB (Eq^n 8). The electrons on the surface of DG simultaneously trap dissolved molecular oxygen and lead to the formation of superoxide radical anions ($O•^{2-}$) (Eq^n 9). Superoxide radical anions directly interact with water molecules to form •OH (Eq^n 10–12). Similarly, the holes (H^+) can be in contact with water molecules producing •OH (Eq^n 13). •OH decomposes simazine pesticides into nontoxic inorganic molecules and ions [181].

There are few recent studies on the removal of heavy metal ions by nanozyme, but there are still several methods with high removal efficiency. AgRu bimetal mesoporous nanozyme costabilized by β-CD and GO (AgRu@ β-CD co GO) was first constructed [168]. The nanozyme has a porous microstructure and a large number of hydroxyl and GO aromatic rings, which can enrich and adsorb a large amount of Hg^+ and Cl^- in water. The authors, through a 0.22 μm commercial millipore filtration membrane, repeatedly filtered the mixed solution containing Hg^+, Cl^-, and nanozyme three times, and the $Hg2^+$ and Cl^- removal efficiency reached more than 95.4% and 93.8%, respectively. In another work, Su et al. [167] investigated the microbial sensitivity regulation mechanism (MSRM) on typical paddy field heavy metal pollution (As^{3+} and Cr^{6+}) using nanozyme nanoMn_3O_4-coated microbial populations (NMCMP) and proved that Flavoisolibacter and Arthrobacter were two main bacteria related to heavy metal (As^{3+} and Cr^{6+}) pollution remediation. In addition, NMCMP can enhance the reduction of Cr^{6+} level and inhibit the release and rapid oxidation of As^{3+} during the repair process of $As_2H_2S_3$ (Figure 8b). Methyl orange is a typical dye in industrial wastewater selected as a typical dye pollutant because it is not easily degraded. CNZ was applied to the degradation of methyl orange pollutants [160]. At a high temperature of 60 °C and pH value of 3.93%, the degradation rate can be obtained in less than 10 minutes. In addition, the nanozyme showed excellent reusability and storage stability. However, Pd@ZnNi-MOF/GO nanocomposites with high peroxidase-like activity took only 8 min to completely degrade the methyl blue dye, and the catalytic degradation efficiency was as high as 95% [162].

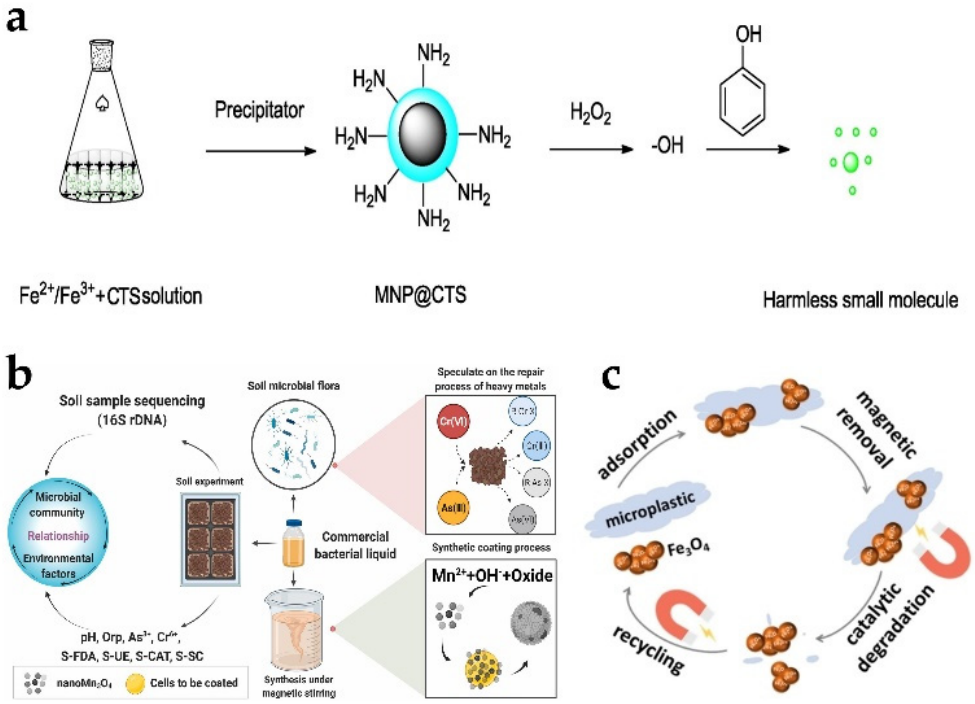

Figure 8. (**a**) Schematic diagram of MNP@CTS nanozyme-catalyzed degradation of phenol [171]. (**b**) Experimental design and process on NMCMP (NMCMP: nanozyme $nanoMn_3O_4$-coated microbial populations) [167]. (**c**) Schematic diagram of Fe_3O_4 nanozyme-catalyzed degradation of microplastics [177]. Reproduced with permission from (**a**) Ref. [171], Copyright 2018 Elsevier; (**b**) Ref. [167], Copyright 2022 Elsevier; (**c**) Ref. [177], Copyright 2022 Wiley Online Library.

Decomposition of phenol and phenolic compound purification of the environment is the focus of social attention. The degradation of phenol and phenolic compounds using ferromagnetic nanoparticles (MNPs) has many advantages. Ferromagnetic chitosan nanozymes (MNP@CTS) have the ability to catalyze the production of reactive oxygen species from hydrogen peroxide. Under the action of reactive oxygen species, the substrate phenol can be rapidly oxidized into various small molecules. Meanwhile, CTS can improve the catalytic efficiency and increase the degradation rate and degradation effect (Figure 8a). The removal efficiency is higher than 95% within 5 h [171]. Microplastics have a high surface-to-volume ratio, and they can act as a carrier for invading microorganisms, heavy metals, and other contaminants. Some of the long-term deleterious effects of microplastics include infertility, degradation of microplastics, and cancer. Therefore, it is crucial to remove and degrade microplastics in water resources. Hydrophilic bare Fe_3O_4 nanoaggregates allowed efficient removal of the most common microplastics including high-density polyethylene, polypropylene, polyvinyl chloride, polystyrene, and polyethylene terephthalate [177]. The bare Fe_3O_4 nanoaggregates with peroxidase-like activity further catalyzed the degradation of microplastics with nearly 100% efficiency by adsorbing to microplastics via hydrogen bonding (Figure 8c).

6. Other Environmental Protection Applications

6.1. Air Purification

Air pollution does great harm to people who breathe with their lungs. Formaldehyde is particularly harmful. Newly decorated rooms often face the problem of too much formaldehyde and cannot be occupied. Ecological nanozymes can catalyze the decomposition of formaldehyde. The average purification rate of formaldehyde in two hours was 91.9% [57]. The composite material is made of activated carbon fiber (ACF) and porous polymer composite and is also equipped with an antibacterial agent. When formaldehyde molecules are sucked into the nanospace, the nanozyme will react with the oxygen in the

air to produce highly active superoxide ions with active oxygen structure. Due to the large contact area between the ecological enzyme catalyst and the adsorbed formaldehyde molecules in the nanopores, the active catalyst molecules quickly combine with formaldehyde molecules. After a series of oxidation-reduction enzyme catalyzed reactions, different peroxyintermediate oxidation molecules are formed. Finally, the formaldehyde molecules are oxidized into water and carbon dioxide molecules [57]. However, the ecological enzyme quickly returned to its original state and combined with oxygen molecules in the air again. The process of "combination with oxygen molecules– formation of active oxygen molecules–combination with formaldehyde molecules–enzymatic decomposition" keeps repeating so as to remove formaldehyde, bacteria, and other organic molecules in the air. This can keep the composite material clean for a long time.

6.2. Antibacterial and Antifouling Agent

Marine biofouling refers to the process in which marine microorganisms, animals, and plants continuously enrich and grow on artificial surfaces to form biofouling, which is a worldwide problem affecting maritime transport and communication facilities and coastal power plants [183]. The microfouling organisms on the substrate surface form a heterogeneous biofilm, which is composed of a variety of heterotrophic bacteria, cyanobacteria, diatoms, protozoa, and fungi [184]. Biofouling can increase hull roughness and weight, increase navigation resistance, greatly increase fuel consumption, cause economic losses of billions of dollars every year, increase carbon dioxide emissions, and intensify the room temperature effect [185]. In addition, organisms attached to distant ships will enter different sea areas, causing potential "species invasion" and affecting the marine ecological balance. When they block the mesh of mariculture cages, they can cause large-scale death of fish and shrimp. For a long time, the method to solve the pollution of marine organisms mainly depended on the toxic effect of heavy metal ions, which also causes serious pollution of the marine environment. In recent years, the research and development of nanozyme provides a new solution to prevent and remove marine biological fouling.

A semiconducting nanozyme consisting of chromium single atoms coordinated on carbon nitride (Cr-SA-CN) that performs bifunctional roles of nonsacrificial H_2O_2 photosynthesis and haloperoxidase-mimicking activity for antibiofouling was constructed [186]. The bifunctional Cr-SA-CN nanoplatform promotes the sustainable formation of HOBr under visible light radiation, so it has excellent antibacterial ability. Moreover, the nanozyme can continuously produce H_2O_2 from underwater and oxygen under visible light irradiation for enzymatic reaction. Field tests in seawater show that Cr-SA-CN, as an antibacterial additive for environmental protection coatings, can prevent the colonization of marine microorganisms on inert surfaces. In addition, the disinfection efficiency of Cr-SA-CN + Br^- against Escherichia coli, Staphylococcus aureus, Pseudomonas aeruginosa, and Vibrio vulnificus was, respectively, 97%, 96%, 92%, and 95%. This study not only proved the ability of monatomic nanozyme to resist biological pollution and sterilization but also provided a strategy for designing more innovative nanozymes with multifunctionality. Nanozyme antifouling agents with the same principle also include photothermal nanozyme with Mo single atom as the active site (Mo SA-N/C), which also has halogen oxide enzyme-like activity [187]. It catalyzes the oxidation of Br^- and H_2O_2 to produce cytotoxic HOBr. At the same time, the photothermal effect induced by visible light greatly accelerates the reaction process. Attapulgite (ATP) is a kind of natural and available nanomineral that has a special layered chain structure, large specific surface area, strong adsorption capacity, and surface dynamic properties. It provides rapid mass transfer and abundant accessible sites for efficient catalytic reactions [188]. Feng et al. [189] synthesized iron and copper-doped ATP (Fe Cu/ATP) with POD-like activity. The addition of Fe and Cu improves the conversion efficiency of H_2O_2, thus showing enhanced POD-like activity. The bactericidal mechanism is to produce reactive oxygen species to attack bacterial populations (Figure 9a). The antibacterial rate of Fe Cu/ATP against Escherichia coli and Staphylococcus aureus is 100% and has a long-term effect. Wei et al. [190] synthesized Fe_3O_4@MoS_2-Ag made great

efforts in bacterial adsorption and toxic attack. Topological structure of MoS_2 nanosheets and S-vacancy enabled Fe_3O_4@MoS_2-Ag to have strong adhesion with bacteria by forming chemical bonds, which shortens the diffusion distance of free radicals and enhances the antibacterial effect (Figure 9b). The nanocomposite has the characteristics of peroxidase simulation and can catalyze H_2O_2 to produce living oxygen to attack bacteria. In addition, the released Ag^+ plays an auxiliary role while attacking the bacterial membrane. Under near-infrared radiation, local hyperthermia and peroxidase simulation can further enhance the sterilization effect. Magnetism also makes it reusable. The method has broad-spectrum antibacterial performance against Gram-negative bacteria, Gram-positive bacteria, drug-resistant bacteria, and fungal bacteria.

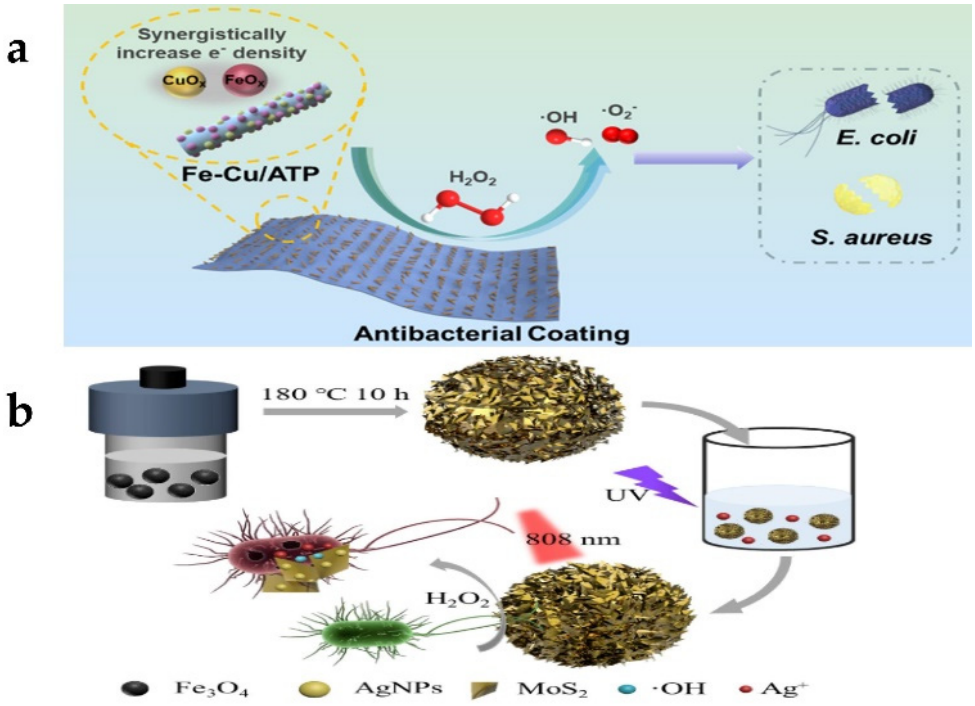

Figure 9. (**a**) Attapulgite doped with Fe and Cu nanooxides as peroxidase nanozymes for antibacterial coatings [189]. (**b**) The schematic preparation of Fe_3O_4@MoS_2-Ag with antibacterial function [190]. Reproduced with permission from (**a**) Ref. [189], Copyright 2022 American Chemical Society; (**b**) Ref. [190], Copyright 2021 Elsevier.

6.3. Enzyme-like Nanomaterial (Nanozyme)-Based Biofuel Cells

Human beings are facing environmental problems caused by the excessive exploitation of fossil energy. In recent years, countries all over the world have focused on sustainable and environment-friendly new energy. Biofuel cells have become an alternative energy conversion device [191]. Biofuel cells can be divided into three categories: microbial biofuel cells (MBFC), enzyme biofuel cells (EBFC), and enzyme-like nanomaterial (nanozymes)-based biofuel cells (NBFC). MBFC have many advantages in waste treatment and environmental protection [192], but the key disadvantage limiting their wide application and commercialization is that their power output is significantly low, and they are extremely difficult to control the internal electron transfer of microorganisms. Unlike MBFC, EBFC catalyze the oxidation of biofuels to generate electricity with the help of natural enzymes. The biofuels of EBFC are usually sugar relatives, such as glucose, sucrose, fructose, alcohols (including ethanol and methanol), organic acids, and organic salts (such as sulfite). However, glucose-based EBFC have many limitations derived from natural enzymes, such as variability and instability, high production cost, and difficult electron transfer [193,194]. In this case, compared with natural enzymes, nanozymes have become potential catalytic materials for developing glucose biofuel cells due to their inherent characteristics (such as long-term

stability, easy synthesis, low cost, and adjustable enzyme mimic activity). Gu et al. [195] found that black phosphorus (BP) showed glucose dehydrogenase (GDH)-like activity and could catalyze the oxidation of glucose without any by-products. BP is a strong alternative candidate for sustainable biofuel cells. Finally, nanozyme-based EBFC consisting of BP anodes for glucose oxidation and Cu^{2+}/carbon nanotube (Cu^{2+}/CNT) cathodes for reducing O_2 under natural conditions were successfully constructed (Figure 10a). The power output of BP-based EBFC is higher than that of GDH-based EBFC. BP nanosheets maintained structural integrity before 360 °C, while the protein structure of GDH was destroyed after 250 °C. More important, EBFC based on nanozyme still showed high stability after 30 days of operation. This work provides more possibilities for the application of BP in the field of nanozyme. Compared with metal-based nanozymes, metal oxide nanozymes can be easily synthesized at low cost. Ho et al. [196] proposed interesting NBFC based on metal oxides, in which $CoMn_2O_4$/carbon was used as a GOx-like anode catalyst in biofuel cell systems. NBFC show a power output of 2.372 mW/cm^2, which is comparable to the commercial platinum/carbon-based biofuel cell system.

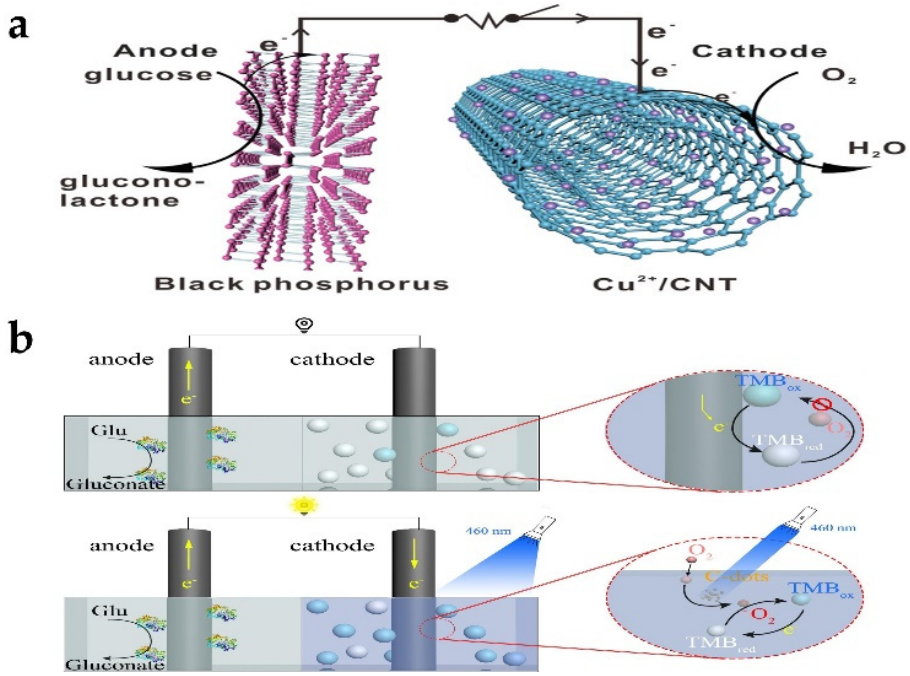

Figure 10. (**a**) Schematic illustration of the as-constructed EBFCs based on BP anode for glucose oxidation and Cu^{2+}/CNT cathode for O_2 reduction [195]. (**b**) Diagram of the photo-switch working mechanism based on C-dots and TMB [197]. Reproduced with permission from (**a**) Ref. [195], Copyright 2020 American Chemical Society; (**b**) Ref. [197], Copyright 2022 Elsevier.

In the traditional design of EBFC, once the fuel is added to the anode, the generation of electric energy will start and continue until the fuel is exhausted or the circuit is cut off. This uncontrollable way will lead to energy waste when EBFC are not used. Li et al. [197] proposed a novel optical switch for EBFC by controlling the electron acceptor in the cathode. When the stable TMBred was oxidized by singlet oxygen activated by the C point under light conditions, the medium can accept the electrons generated by the enzyme anode, thus leading to the formation of a path for the external circuit. Without radiation, TMBred cannot be converted into TMB198ox. A limited amount of electron acceptors is rapidly depleted, resulting in almost zero current and power density. Here, the C-point nanozyme was used as a photosensitizer of oxygen, and TMB is added to the cathode chamber as an electron acceptor. Theoretically, without lighting, there should be no current in the external circuit, showing a completely "off" state. The EBFC can be precisely and easily adjusted by the optical switch with light as the input signal (Figure 10b). Therefore, it avoids the

damage to the anode enzyme caused by the traditional pH switch. This optical switch can adjust the power output of EBFC according to specific optical signals and promote the "intelligent" application of EBFC.

Enzymes such as nanomaterial (nanozyme)-based biofuel cells mainly use noble metal-based nanozymes, metal oxide-based nanozymes, and electron-receiving laccase that can mimic natural GOx and catalase. NBFC are stable and have a long service life. The high catalytic activity of glucose oxidation can output enough power, which can be synthesized on a large scale and has low production cost. The use of nanozymes in glucose biofuel cell systems has significantly improved the power generation performance. The utilization of NBFC will continue to improve.

7. Conclusions and Prospects

To summarize, we reviewed the application of nanozyme in the environmental field from three aspects: environmental monitoring, environmental management, and other environmental applications. The influencing factors of nanozyme catalytic activity were briefly summarized as well. The size, structure, composition combination, doping, and surface modification of nanozyme can adjust the catalytic activity of nanozyme. The specificity of nanozyme is mainly improved by biological recognition molecules (biological enzyme, MIP, DNA, antibody, aptamer) and the simulation of the active center and binding site of the biological enzyme. In addition to its own intrinsic enzyme activity, it can also affect the catalytic efficiency through pH, temperature, light stimulation, and so on. In terms of environmental monitoring and treatment, the detection and degradation of heavy metal ions, phenolic compounds, dyes, plasticizers, pesticides, and antibiotics all involve nanozymes. Moreover, nanozymes can be used as antibacterial and antifouling agents and biofuel cells to indirectly protect the environment. Great development and applications of nanozyme have been promoted in the field of environmental science.

Nanozyme has been developed for more than 20 years. Nanomaterials with new enzyme activities have been continuously explored. The design strategy of nanozymes has been constantly improved. However, nanozyme still has some limitations regarding the direction of development in the future.

- At present, the types of nanozymes are still too few, and they are mainly concentrated in the oxidoreductase family and hydrolase family. Compared with the six categories of natural enzymes, there is still an urgent need to unlock more simulated enzymes with different catalytic activities to expand the scope of application.
- Nanozymes are a succedaneum for natural enzymes, but the catalytic activity of most nanozymes is far inferior to natural enzymes. Hence, strategies need to be continuously explored to improve their catalytic activity.
- Nanozymes can show good performance in the laboratory. Nevertheless, they are still disadvantaged because they cannot be used on a large scale for the actual pollutant treatment industry, such as catalytic devices requiring high-precision technology, short service life, and higher cost than traditional environmental treatment methods.
- Although some nanozymes that break through the restriction of pH have appeared, most nanozymes are still limited by pH with narrow range. Technological breakthroughs are still needed in this regard so that the catalytic activity of most nanozymes is no longer limited by pH.
- Nanozymes are intrinsically toxic. It is vital to design low-toxicity nanozymes by adjusting their physical and chemical properties such as size, shape, surface properties, surface charge, and chemical composition to avoid secondary contamination.
- In recent years, nanozymes with multienzyme activity have been continuously developed, which can be used for multifunctional applications. However, at the same time, facing the challenge that the selectivity of nanozymes with multienzyme activity is lower than that of single-enzyme live nanozymes, will

challenge researchers to balance the relationship between "multifunction" and "high selectivity" as well as achieve a win–win situation.

- Recently, the specificity of nanozyme is much lower than that of natural enzyme. The design of nanozyme should be committed to better a bionic biological enzyme's active center and binding site, and the recognition element should be stably and effectively connected to the nanozyme. In addition, it is critical to explore the mechanism and law of interactions between nanozyme and a recognition element. Meanwhile, it is still necessary to improve the performance of nanozyme sensors by combining the research results of specific recognition in other fields and sensing technologies.
- Nanozyme detection mostly relies on colorimetric sensing, but colorimetric sensing has the problems of large interference and low sensitivity. In addition to electrochemistry, photoelectrochemistry, and surface-enhanced Raman scattering (SERS), adding more detection modes can have unexpected effects on environmental monitoring.

Author Contributions: M.W.: Conceptualization, Writing—Original Draft Preparation; P.Z.: Writing—Review and Editing, Visualization; S.L.: Writing—Review and Editing; Y.C.: Writ-ing—Review and Editing; D.L.: Conceptualization, Writing—Review and Editing; Y.L.: Writing—Review and Editing; W.C.: Concep-tualization, Writing—Review and Editing; L.D.: Conceptualization, Writing—Review and Edit-ing; Supervision, Funding Acquisition; C.W.: Writing—Review and Editing; Supervision, Funding Acquisition; Project Administration. All authors have read and agreed to the published version of the manuscript.

Funding: This research was funded by the Key Research and Development Program of Shaanxi Province-International Science and Technology Cooperation General Project (Grant No. 2022KW-23), the National Natural Science Foundation of China (Grant No. 32071370, 51861145307, and 32271427), and the Chunhui Research Grant of the Ministry of Education of China.

Institutional Review Board Statement: No human participants and/or animals were used for the research.

Informed Consent Statement: No human participants and/or animals were used for the research.

Conflicts of Interest: The authors declare that they have no known competing financial interest or personal relationships that could have appeared to influence the work reported in this paper.

References

1. Van Beilen, J.B.; Li, Z. Enzyme technology: An overview. *Curr. Opin. Biotechnol.* **2002**, *13*, 338–344. [CrossRef]
2. Jaeger, K.E.; Eggert, T. Enantioselective biocatalysis optimized by directed evolution. *Curr. Opin. Biotechnol.* **2004**, *15*, 305–313. [CrossRef]
3. Huang, W.; Huang, S.M.; Chen, G.S.; Ouyang, G.F. Biocatalytic Metal-Organic Frameworks: Promising Materials for Biosensing. *Chembiochem* **2022**, *23*, e202100567. [CrossRef] [PubMed]
4. Garcia-Galan, C.; Berenguer-Murcia, A.; Fernandez-Lafuente, R.; Rodrigues, R.C. Potential of Different Enzyme Immobilization Strategies to Improve Enzyme Performance. *Adv. Synth. Catal.* **2011**, *353*, 2885–2904. [CrossRef]
5. Breslow, R.; Baldwin, S.W. Conversion of cholestanol to 12-ketocholestanol and to delta14-cholestenol and delta8(14)-cholestenol by remote oxidation. *J. Am. Chem. Soc.* **1970**, *92*, 732–734. [CrossRef]
6. Manea, F.; Houillon, F.B.; Pasquato, L.; Scrimin, P. Nanozymes: Gold-nanoparticle-based transphosphorylation catalysts. *Angew. Chem. Int. Ed.* **2004**, *43*, 6165–6169. [CrossRef] [PubMed]
7. Gao, L.Z.; Zhuang, J.; Nie, L.; Zhang, J.B.; Zhang, Y.; Gu, N.; Wang, T.H.; Feng, J.; Yang, D.L.; Perrett, S.; et al. Intrinsic peroxidase-like activity of ferromagnetic nanoparticles. *Nat. Nanotechnol.* **2007**, *2*, 577–583. [CrossRef]
8. Wei, H.; Wang, E.K. Nanomaterials with enzyme-like characteristics (nanozymes): Next-generation artificial enzymes. *Chem. Soc. Rev.* **2013**, *42*, 6060–6093. [CrossRef]
9. Jiang, B.; Duan, D.M.; Gao, L.Z.; Zhou, M.J.; Fan, K.L.; Tang, Y.; Xi, J.Q.; Bi, Y.H.; Tong, Z.; Gao, G.F.; et al. Standardized assays for determining the catalytic activity and kinetics of peroxidase-like nanozymes. *Nat. Protoc.* **2018**, *13*, 1506–1520. [CrossRef]
10. Iswarya, V.; Johnson, J.B.; Parashar, A.; Pulimi, M.; Chandrasekaran, N.; Mukherjee, A. Modulatory effects of Zn^{2+} ions on the toxicity of citrate-and PVP-capped gold nanoparticles towards freshwater algae, Scenedesmus obliquus. *Environ. Sci. Pollut. Res.* **2017**, *24*, 3790–3801. [CrossRef]

11. Lv, X.; Yang, Y.; Tao, Y.; Jiang, Y.; Chen, B.; Zhu, X.; Cai, Z.; Li, B. A mechanism study on toxicity of graphene oxide to Daphnia magna: Direct link between bioaccumulation and oxidative stress. *Environ. Pollut.* **2018**, *234*, 953–959. [CrossRef] [PubMed]
12. Albanese, A.; Tang, P.S.; Chan, W.C.W. The Effect of Nanoparticle Size, Shape, and Surface Chemistry on Biological Systems. *Annu. Rev. Biomed. Eng.* **2012**, *14*, 1–16. [CrossRef] [PubMed]
13. Liu, Y.; Li, W.; Lao, F.; Liu, Y.; Wang, L.; Bai, R.; Zhao, Y.; Chen, C. Intracellular dynamics of cationic and anionic polystyrene nanoparticles without direct interaction with mitotic spindle and chromosomes. *Biomaterials* **2011**, *32*, 8291–8303. [CrossRef] [PubMed]
14. Rasmussen, M.K.; Pedersen, J.N.; Marie, R. Size and surface charge characterization of nanoparticles with a salt gradient. *Nat. Commun.* **2020**, *11*, 2337. [CrossRef] [PubMed]
15. Gahlawat, G.; Choudhury, A.R. A review on the biosynthesis of metal and metal salt nanoparticles by microbes. *RSC Adv.* **2019**, *9*, 12944–12967. [CrossRef]
16. Zhang, M.; Qu, Y.; Li, D.X.; Liu, X.Y.; Niu, Y.S.; Xu, Y.H. To Love and to Kill: Accurate and Selective Colorimetry for Both Chloride and Mercury Ions Regulated by Electro-Synthesized Oxidase-like SnTe Nanobelts. *Anal. Chem.* **2021**, *93*, 10132–10140. [CrossRef]
17. Liang, X.; Han, L. White Peroxidase-Mimicking Nanozymes: Colorimetric Pesticide Assay without Interferences of O-2 and Color. *Adv. Funct. Mater.* **2020**, *30*, 2001933. [CrossRef]
18. Xu, D.; Wu, L.; Yao, H.; Zhao, L. Catalase-Like Nanozymes: Classification, Catalytic Mechanisms, and Their Applications. *Small* **2022**, *18*, 2203400. [CrossRef] [PubMed]
19. Li, X.; Zhu, H.; Liu, P.; Wang, M.; Pan, J.; Qiu, F.; Ni, L.; Niu, X. Realizing selective detection with nanozymes: Strategies and trends. *TrAC Trends Anal. Chem.* **2021**, *143*, 116379. [CrossRef]
20. Golchin, J.; Golchin, K.; Alidadian, N.; Ghaderi, S.; Eslamkhah, S.; Eslamkhah, M.; Akbarzadeh, A. Nanozyme applications in biology and medicine: An overview. *Artif. Cells Nanomed. Biotechnol.* **2017**, *45*, 1069–1076. [CrossRef]
21. Jiang, L.; Sun, Y.; Chen, Y.; Nan, P. From DNA to Nerve Agents—The Biomimetic Catalysts for the Hydrolysis of Phosphate Esters. *Chemistryselect* **2020**, *5*, 9492–9516. [CrossRef]
22. Ballesteros, C.A.S.; Mercante, L.A.; Alvarenga, A.D.; Facure, M.H.M.; Schneider, R.; Correa, D.S. Recent trends in nanozymes design: From materials and structures to environmental applications. *Mater. Chem. Front.* **2021**, *5*, 7419–7451. [CrossRef]
23. Ye, N.R.; Huang, S.M.; Yang, H.S.; Wu, T.; Tong, L.J.; Zhu, F.; Chen, G.S.; Ouyang, G.F. Hydrogen-Bonded Biohybrid Framework-Derived Highly Specific Nanozymes for Biomarker Sensing. *Anal. Chem.* **2021**, *93*, 13981–13989. [CrossRef]
24. Cai, R.; Liu, J.B.; Wu, X.C. Research Progress of Noble Metal-based Nanozymes. *Chem. J. Chin. Univ. Chin.* **2021**, *42*, 1188–1201. [CrossRef]
25. Cai, S.; Yang, R. Noble Metal-Based Nanozymes. In *Nanozymology. Nanostructure Science and Technology*; Springer: Singapore, 2020; pp. 331–365.
26. Cai, Z.; Kuang, Y.; Qi, X.; Wang, P.; Zhang, Y.; Zhang, Z.; Sun, X. Ultrathin branched PtFe and PtRuFe nanodendrites with enhanced electrocatalytic activity. *J. Mater. Chem. A* **2015**, *3*, 1182–1187. [CrossRef]
27. Liu, Q.; Zhang, A.; Wang, R.; Zhang, Q.; Cui, D. A Review on Metal- and Metal Oxide-Based Nanozymes: Properties, Mechanisms, and Applications. *Nano-Micro Lett.* **2021**, *13*, 154. [CrossRef]
28. Liang, B.; Li, B.; Li, Z.Q.; Chen, B.L. Progress in Multifunctional Metal-Organic Frameworks/Polymer Hybrid Membranes. *Chem. A Eur. J.* **2021**, *27*, 12940–12952. [CrossRef] [PubMed]
29. Huang, X.; Zhang, S.T.; Tang, Y.J.; Zhang, X.Y.; Bai, Y.; Pang, H. Advances in metal-organic framework-based nanozymes and their applications. *Coord. Chem. Rev.* **2021**, *449*, 214216. [CrossRef]
30. Meng, W.; Liu, X.; Song, H.; Xie, Y.; Shi, X.; Dargusch, M.; Chen, Z.-G.; Tang, Z.; Lu, S. Advances and challenges in 2D MXenes: From structures to energy storage and conversions. *Nano Today* **2021**, *40*, 101273. [CrossRef]
31. Li, M.M.; Peng, X.Y.; Han, Y.J.; Fan, L.F.; Liu, Z.G.; Guo, Y.J. Ti_3C_2 MXenes with intrinsic peroxidase-like activity for label-free and colorimetric sensing of proteins. *Microchem. J.* **2021**, *166*, 106238. [CrossRef]
32. Li, S.R.; Zhang, Y.H.; Wang, Q.; Lin, A.Q.; Wei, H. Nanozyme-Enabled Analytical Chemistry. *Anal. Chem.* **2022**, *94*, 312–323. [CrossRef]
33. Valden, M.; Lai, X.; Goodman, D.W. Onset of catalytic activity of gold clusters on titania with the appearance of nonmetallic properties. *Science* **1998**, *281*, 1647–1650. [CrossRef] [PubMed]
34. Zhou, X.C.; Xu, W.L.; Liu, G.K.; Panda, D.; Chen, P. Size-Dependent Catalytic Activity and Dynamics of Gold Nanoparticles at the Single-Molecule Level. *J. Am. Chem. Soc.* **2010**, *132*, 138–146. [CrossRef]
35. Kalantari, M.; Ghosh, T.; Liu, Y.; Zhang, J.; Zou, J.; Lei, C.; Yu, C.Z. Highly Thiolated Dendritic Mesoporous Silica Nanoparticles with High-Content Gold as Nanozymes: The Nano-Gold Size Matters. *Acs Appl. Mater. Interfaces* **2019**, *11*, 13264–13272. [CrossRef]
36. Biswas, S.; Tripathi, P.; Kumar, N.; Nara, S. Gold nanorods as peroxidase mimetics and its application for colorimetric biosensing of malathion. *Sens. Actuators B-Chem.* **2016**, *231*, 584–592. [CrossRef]
37. Tian, R.; Sun, J.H.; Qi, Y.F.; Zhang, B.Y.; Guo, S.L.; Zhao, M.M. Influence of VO_2 Nanoparticle Morphology on the Colorimetric Assay of H_2O_2 and Glucose. *Nanomaterials* **2017**, *7*, 347. [CrossRef] [PubMed]
38. Wu, J.J.X.; Wang, X.Y.; Wang, Q.; Lou, Z.P.; Li, S.R.; Zhu, Y.Y.; Qin, L.; Wei, H. Nanomaterials with enzyme-like characteristics (nanozymes): Next-generation artificial enzymes (II). *Chem. Soc. Rev.* **2019**, *48*, 1004–1076. [CrossRef]

39. Zhu, W.; Cheng, Y.; Yan, S.; Chen, X.; Wang, C.; Lu, X. A general cation-exchange strategy for constructing hierarchical TiO_2/$CuInS_2$/CuS hybrid nanofibers to boost their peroxidase-like activity toward sensitive detection of dopamine. *Microchem. J.* **2022**, *183*, 108090. [CrossRef]
40. Feng, X.Y.; Fu, H.; Bai, Z.Y.; Li, P.; Song, X.L.; Hu, X.P. Colorimetric detection of glucose by a hybrid nanomaterial based on amplified peroxidase-like activity of ferrosoferric oxide modified with gold-platinum heterodimer. *New J. Chem.* **2021**, *46*, 239–249. [CrossRef]
41. Zhao, L.; Ren, X.; Zhang, J.; Zhang, W.; Chen, X.; Meng, X. Dendritic silica with carbon dots and gold nanoclusters for dual nanozymes. *New J. Chem.* **2020**, *44*, 1988–1992. [CrossRef]
42. Liu, B.W.; Liu, J.W. Surface modification of nanozymes. *Nano Res.* **2017**, *10*, 1125–1148. [CrossRef]
43. Lee, A.H.Y.; Kang, W.S.; Choi, J.S. Highly Enhanced Enzymatic Activity of Mn-Induced Carbon Dots and Their Application as Colorimetric Sensor Probes. *Nanomaterials* **2021**, *11*, 3046. [CrossRef] [PubMed]
44. Sun, S.X.; Zhang, Z.J.; Xiang, Y.; Cao, M.W.; Yu, D.Y. Amino Acid-Mediated Synthesis of the ZIF-8 Nanozyme That Reproduces Both the Zinc-Coordinated Active Center and Hydrophobic Pocket of Natural Carbonic Anhydrase. *Langmuir* **2022**, *38*, 1621–1630. [CrossRef] [PubMed]
45. Jain, V.; Bhagat, S.; Singh, M.; Bansal, V.; Singh, S. Unveiling the effect of 11-MUA coating on biocompatibility and catalytic activity of a gold-core cerium oxide-shell-based nanozyme. *RSC Adv.* **2019**, *9*, 33195–33206. [CrossRef] [PubMed]
46. Gao, L.Z.; Liu, Y.; Kim, D.; Li, Y.; Hwang, G.; Naha, P.C.; Cormode, D.P.; Koo, H. Nanocatalysts promote Streptococcus mutans biofilm matrix degradation and enhance bacterial killing to suppress dental caries in vivo. *Biomaterials* **2016**, *101*, 272–284. [CrossRef]
47. Li, D.D.; Guo, Q.Q.; Ding, L.M.; Zhang, W.; Cheng, L.; Wang, Y.Q.; Xu, Z.B.; Wang, H.H.; Gao, L.Z. Bimetallic $CuCo_2S_4$ Nanozymes with Enhanced Peroxidase Activity at Neutral pH for Combating Burn Infections. *Chembiochem* **2020**, *21*, 2620–2627. [CrossRef]
48. Chen, J.X.; Huang, L.; Wang, Q.Q.; Wu, W.W.; Zhang, H.; Fang, Y.X.; Dong, S.J. Bio-inspired nanozyme: A hydratase mimic in a zeolitic imidazolate framework. *Nanoscale* **2019**, *11*, 5960–5966. [CrossRef]
49. Li, M.H.; Chen, J.X.; Wu, W.W.; Fang, Y.X.; Dong, S.J. Oxidase-like MOF-818 Nanozyme with High Specificity for Catalysis of Catechol Oxidation. *J. Am. Chem. Soc.* **2020**, *142*, 15569–15574. [CrossRef]
50. Xu, B.L.; Wang, H.; Wang, W.W.; Gao, L.Z.; Li, S.S.; Pan, X.T.; Wang, H.Y.; Yang, H.L.; Meng, X.Q.; Wu, Q.W.; et al. A Single-Atom Nanozyme for Wound Disinfection Applications. *Angew. Chem.-Int. Ed.* **2019**, *58*, 4911–4916. [CrossRef]
51. Chen, L.X.; Xu, S.F.; Li, J.H. Recent advances in molecular imprinting technology: Current status, challenges and highlighted applications. *Chem. Soc. Rev.* **2011**, *40*, 2922–2942. [CrossRef]
52. Zhang, Z.J.; Zhang, X.H.; Liu, B.W.; Liu, J.W. Molecular Imprinting on Inorganic Nanozymes for Hundred-fold Enzyme Specificity. *J. Am. Chem. Soc.* **2017**, *139*, 5412–5419. [CrossRef] [PubMed]
53. Li, W.S.; Fan, G.C.; Gao, F.X.; Cui, Y.G.; Wang, W.; Luo, X.L. High-activity Fe_3O_4 nanozyme as signal amplifier: A simple, low-cost but efficient strategy for ultrasensitive photoelectrochemical immunoassay. *Biosens. Bioelectron.* **2019**, *127*, 64–71. [CrossRef] [PubMed]
54. Chau, L.Y.; He, Q.; Qin, A.; Yip, S.P.; Lee, T.M.H. Platinum nanoparticles on reduced graphene oxide as peroxidase mimetics for the colorimetric detection of specific DNA sequence. *J. Mater. Chem. B* **2016**, *4*, 4076–4083. [CrossRef] [PubMed]
55. Liu, B.; Liu, J. Accelerating peroxidase mimicking nanozymes using DNA. *Nanoscale* **2015**, *7*, 13831–13835. [CrossRef] [PubMed]
56. Zhu, X.; Tang, L.; Wang, J.J.; Peng, B.; Ouyang, X.L.; Tan, J.S.; Yu, J.F.; Feng, H.P.; Tang, J.L. Enhanced peroxidase-like activity of boron nitride quantum dots anchored porous CeO_2 nanorods by aptamer for highly sensitive colorimetric detection of kanamycin. *Sens. Actuators B-Chem.* **2021**, *330*, 129318. [CrossRef]
57. Meng, Y.T.; Li, W.F.; Pan, X.L.; Gadd, G.M.G. Applications of nanozymes in the environment. *Environ. Sci. Nano* **2020**, *7*, 1305–1318. [CrossRef]
58. Wang, Y.; Wang, Y.; Wang, F.; Chi, H.; Zhao, G.; Zhang, Y.; Li, T.; Wei, Q. Electrochemical aptasensor based on gold modified thiol graphene as sensing platform and gold-palladium modified zirconium metal-organic frameworks nanozyme as signal enhancer for ultrasensitive detection of mercury ions. *J. Colloid Interface Sci.* **2022**, *606*, 510–517. [CrossRef]
59. Tian, H.; Liu, J.; Guo, J.; Cao, L.; He, J. L-Cysteine functionalized graphene oxide nanoarchitectonics: A metal-free Hg^{2+} nanosensor with peroxidase-like activity boosted by competitive adsorption. *Talanta* **2022**, *242*, 123320. [CrossRef]
60. Zhong, X.-L.; Wen, S.-H.; Wang, Y.; Luo, Y.-X.; Li, Z.-M.; Liang, R.-P.; Zhang, L.; Qiu, J.-D. Colorimetric and electrochemical arsenate assays by exploiting the peroxidase-like activity of FeOOH nanorods. *Microchim. Acta* **2019**, *186*, 732. [CrossRef]
61. Zhang, Y.; Zhao, T.; Zhang, X.; Akhtar, M.H.; Zhang, Q.; Li, M.; Yu, C. Photothermal and colorimetric dual-readout silver ions determination utilizing the oxidase-mimicking activity of MnO_2 nanosheets. *Sens. Actuators B Chem.* **2021**, *346*, 130494. [CrossRef]
62. Chen, G.; Jin, M.; Ma, J.; Yan, M.; Cui, X.; Wang, Y.; Zhang, X.; Li, H.; Zheng, W.; Zhang, Y.; et al. Competitive Bio-Barcode Immunoassay for Highly Sensitive Detection of Parathion Based on Bimetallic Nanozyme Catalysis. *J. Agric. Food Chem.* **2020**, *68*, 660–668. [CrossRef] [PubMed]
63. Bagheri, N.; Khataee, A.; Hassanzadeh, J.; Samaei, L. Highly sensitive chemiluminescence sensing system for organophosphates using mimic LDH supported ZIF-8 nanocomposite. *Sens. Actuators B Chem.* **2019**, *284*, 220–227. [CrossRef]
64. Song, P.; Wang, M.; Xue, Y.; Wang, A.-J.; Mei, L.P.; Feng, J.-J. Bimetallic PtNi nanozyme-driven dual-amplified photoelectrochemical aptasensor for ultrasensitive detection of sulfamethazine based on Z-scheme heterostructured Co9S8@In-CdS nanotubes. *Sens. Actuators B Chem.* **2022**, *371*, 132519. [CrossRef]

65. Sun, M.M.; He, M.X.; Jiang, S.J.; Wang, Y.Y.; Wang, X.X.; Liu, T.; Song, C.; Wang, S.N.; Rao, H.B.; Lu, Z.W. Multi-enzyme activity of three layers FeOx@ZnMnFeOy@Fe-Mn organogel for colorimetric detection of antioxidants and norfloxacin with smartphone. *Chem. Eng. J.* **2021**, *425*, 131823. [CrossRef]
66. Liu, X.; Yang, J.; Cheng, J.; Xu, Y.; Chen, W.; Li, Y. Facile preparation of four-in-one nanozyme catalytic platform and the application in selective detection of catechol and hydroquinone. *Sens. Actuators B-Chem.* **2021**, *337*, 129763. [CrossRef]
67. Ma, Y.; Zhu, M.; He, Q.; Zhao, M.; Cui, H. Photoenhanced Oxidase-Peroxidase-like $NiCo_2O_4$@MnO_2 Nanozymes for Colorimetric Detection of Hydroquinone. *ACS Sustain. Chem. Eng.* **2022**, *10*, 5651–5658. [CrossRef]
68. Zhou, J.; Tian, F.; Fu, R.; Yang, Y.; Jiao, B.; He, Y. Enzyme-Nanozyme Cascade Reaction-Mediated Etching of Gold Nanorods for the Detection of Escherichia coli. *ACS Appl. Nano Mater.* **2020**, *3*, 9016–9025. [CrossRef]
69. Hu, J.; Tang, F.; Wang, L.; Tang, M.; Jiang, Y.-Z.; Liu, C. Nanozyme sensor based-on platinum-decorated polymer nanosphere for rapid and sensitive detection of Salmonella typhimurium with the naked eye. *Sens. Actuators B Chem.* **2021**, *346*, 130560. [CrossRef]
70. Wu, S.-C.; Tsai, T.-T.; Li, T.-H.; Tung, C.-Y.; Chiu, P.-Y.; Lin, J.-H.; Chen, C.-F. Palladium-platinum bimetallic nanomaterials and their application in Staphylococcus aureus detection on paper-based devices. *Biosens. Bioelectron.* **2022**, *216*, 114669. [CrossRef]
71. Luo, S.; Liu, F.; Gu, S.; Chen, K.; Yang, G.; Gu, Y.; Cao, J.; Qu, L.-L. Nanozyme-mediated signal amplification for ultrasensitive photoelectrochemical sensing of Staphylococcus aureus based on Cu-C_3N_4-TiO(2)heterostructure. *Biosens. Bioelectron.* **2022**, *216*, 114593. [CrossRef]
72. Zhang, B.; Zou, H.; Qi, Y.; Zhang, X.; Sheng, R.; Zhang, Y.; Sun, R.; Chen, L.; Lv, R. Assembly of polyoxometalates/polydopamine nanozymes as a multifunctional platform for glutathione and *Escherichia coli* O157:H7 detection. *Microchem. J.* **2021**, *164*, 106013. [CrossRef]
73. Xie, D.; Liu, Q.; Wang, J.; Zhang, X.; Gu, K.; Sun, K. Chromogenic reaction of ABTS catalyzed by MnO_2 nanozyae and its application in the visual detection of Fe^{2+} and Pb^{2+}. *Huanjing Huaxue-Environ. Chem.* **2019**, *38*, 2843–2850. [CrossRef]
74. Qiu, Z.W.; Duan, W.; Cao, S.F.; Zeng, T.; Zhao, T.Y.; Huang, J.K.; Lu, X.Q.; Zeng, J.B. Highly Specific Colorimetric Probe for Fluoride by Triggering the Intrinsic Catalytic Activity of a AgPt-Fe_3O_4 Hybrid Nanozyme Encapsulated in SiO_2 Shells. *Environ. Sci. Technol.* **2022**, *56*, 1713–1723. [CrossRef] [PubMed]
75. Adegoke, O.; Zolotovskaya, S.; Abdolvand, A.; Daeid, N.N. Rapid and highly selective colorimetric detection of nitrite based on the catalytic-enhanced reaction of mimetic Au nanoparticle-CeO_2 nanoparticle-graphene oxide hybrid nanozyme. *Talanta* **2021**, *224*, 121875. [CrossRef] [PubMed]
76. Wang, L.J.; Xu, X.C.; Liu, P.; Wang, M.Z.; Niu, X.H.; Pan, J.M. A single-nanozyme colorimetric array based on target-induced differential surface passivation for quantification and discrimination of Cl^-, Br^- and I^- ions. *Anal. Chim. Acta* **2021**, *1160*, 338451. [CrossRef]
77. Hu, S.Y.; Yan, G.H.; Zhang, L.Y.; Yi, S.S.; Zhang, Z.T.; Wang, Y.; Chen, D.L. Highly Selective Colorimetric Detection of Cu^{2+} Using EDTA- Complexed Chlorophyll-Copper/ZnO Nanorods with Cavities Specific to Cu^{2+} as a Light-Activated Nanozyme. *Acs Appl. Mater. Interfaces* **2022**, *14*, 37716–37726. [CrossRef]
78. Xu, X.C.; Wang, L.J.; Zou, X.B.; Wu, S.W.; Pan, J.M.; Li, X.; Niu, X.H. Highly sensitive colorimetric detection of arsenite based on reassembly-induced oxidase-mimicking activity inhibition of dithiothreitol-capped Pd nanozyme. *Sens. Actuators B Chem.* **2019**, *298*, 126876. [CrossRef]
79. Honarasa, F.; Peyravi, F.; Amirian, H. C-dots/Mn_3O_4 nanocomposite as an oxidase nanozyme for colorimetric determination of ferrous ion. *J. Iran. Chem. Soc.* **2020**, *17*, 507–512. [CrossRef]
80. Liu, L.; Du, J.; Liu, W.E.; Guo, Y.L.; Wu, G.F.; Qi, W.N.; Lu, X.Q. Enhanced His@AuNCs oxidase-like activity by reduced graphene oxide and its application for colorimetric and electrochemical detection of nitrite. *Anal. Bioanal. Chem.* **2019**, *411*, 2189–2200. [CrossRef]
81. Shi, Y.; Liu, Z.; Liu, R.; Wu, R.; Zhang, J.J. DNA-encoded MXene-Pt nanozyme for enhanced colorimetric sensing of mercury ions. *Chem. Eng. J.* **2022**, *442*, 136072. [CrossRef]
82. Zhao, J.; Gong, J.W.; Wei, J.N.; Yang, Q.; Li, G.J.; Tong, Y.P.; He, W.W. Metal organic framework loaded fluorescent nitrogen-doped carbon nanozyme with light regulating redox ability for detection of ferric ion and glutathione. *J. Colloid Interface Sci.* **2022**, *618*, 11–21. [CrossRef] [PubMed]
83. Xue, Q.S.; Li, X.; Peng, Y.X.; Liu, P.; Peng, H.B.; Niu, X.H. Polyethylenimine-stabilized silver nanoclusters act as an oxidoreductase mimic for colorimetric determination of chromium(VI). *Microchim. Acta* **2020**, *187*, 263. [CrossRef] [PubMed]
84. Xu, R.X.; Wang, Z.Y.; Liu, S.Q.; Li, H. Bimetallic AuRu aerogel with enzyme-like activity for colorimetric detection of Fe2+ and glucose. *Chin. Chem. Lett.* **2022**, *33*, 4683–4686. [CrossRef]
85. Huang, L.J.; Zhu, Q.R.; Zhu, J.; Luo, L.P.; Pu, S.H.; Zhang, W.T.; Zhu, W.X.; Sun, J.; Wang, J.L. Portable Colorimetric Detection of Mercury(II) Based on a Non-Noble Metal Nanozyme with Tunable Activity. *Inorg. Chem.* **2019**, *58*, 1638–1646. [CrossRef]
86. Lin, L.; Chen, D.X.; Lu, C.F.; Wang, X.X. Fluorescence and colorimetric dual-signal determination of Fe^{3+} and glutathione with $MoSe_2$@Fe nanozyme. *Microchem. J.* **2022**, *177*, 107283. [CrossRef]
87. Wen, S.S.; Zhang, Z.W.; Zhang, Y.P.; Liu, H.; Ma, X.W.; Li, L.J.; Song, W.; Zhao, B. Ultrasensitive Stimulation Effect of Fluoride Ions on a Novel Nanozyme-SERS System. *ACS Sustain. Chem. Eng.* **2020**, *8*, 11906–11913. [CrossRef]

88. Yang, Z.P.; Liu, Y.Q.; Liu, Y.; Wang, Y.Y.; Rao, H.B.; Liu, Y.; Yin, J.J.; Yue, G.Z.; Wu, C.M.; Li, H.; et al. Preparation of porous uranium oxide hollow nanospheres with peroxidase mimicking activity: Application to the colorimetric determination of tin(II). *Microchim. Acta* **2019**, *186*, 501. [CrossRef]
89. Zhang, G.Y.; Yu, K.; Zhou, B.J.; Wang, J.Y.; Zheng, C.; Qu, L.J.; Chai, H.N.; Zhang, X.J. Magnetic zirconium-based Prussian blue analog nanozyme: Enhanced peroxidase-mimicking activity and colorimetric sensing of phosphate ion. *Microchim. Acta* **2022**, *189*, 220. [CrossRef]
90. Xiong, Y.H.; Su, L.J.; Ye, F.G.; Zhao, S.L. Porous Oxyhydroxide Derived from Metal-Organic Frameworks as Efficient Triphosphatase-like Nanozyme for Chromium(III) Ion Colorimetric Sensing. *Acs Appl. Bio Mater.* **2021**, *4*, 6962–6973. [CrossRef]
91. Song, G.C.; Li, J.C.; Majid, Z.; Xu, W.T.; He, X.Y.; Yao, Z.Y.; Luo, Y.B.; Huang, K.L.; Cheng, N. Phosphatase-like activity of single-atom Ce-N-C nanozyme for rapid detection of Al^{3+}. *Food Chem.* **2022**, *390*, 133127. [CrossRef]
92. Goswami, J.; Saikia, L.; Hazarika, P. Carbon Dots-Decorated g-C_3N_4 as Peroxidase Nanozyme for Colorimetric Detection of Cr(VI) in Aqueous Medium. *Chemistryselect* **2022**, *7*, e202201963. [CrossRef]
93. Fang, Y.M.; Zhang, Y.; Cao, L.G.; Yang, J.Z.; Hu, M.H.; Pang, Z.L.; He, J.H. Portable Hg^{2+} Nanosensor with ppt Level Sensitivity Using Nanozyme as the Recognition Unit, Enrichment Carrier, and Signal Amplifier. *Acs Appl. Mater. Interfaces* **2020**, *12*, 11761–11768. [CrossRef]
94. Wen, S.H.; Zhong, X.L.; Wu, Y.D.; Liang, R.P.; Zhang, L.; Qiu, J.D. Colorimetric Assay Conversion to Highly Sensitive Electrochemical Assay for Bimodal Detection of Arsenate Based on Cobalt Oxyhydroxide Nanozyme via Arsenate Absorption. *Anal. Chem.* **2019**, *91*, 6487–6497. [CrossRef]
95. Kulandaivel, S.; Lo, W.C.; Lin, C.H.; Yeh, Y.C. Cu-PyC MOF with oxidoreductase-like catalytic activity boosting colorimetric detection of Cr(VI) on paper. *Anal. Chim. Acta* **2022**, *1227*, 340335. [CrossRef]
96. Amini, R.; Rahimpour, E.; Jouyban, A. An optical sensing platform based on hexacyanoferrate intercalated layered double hydroxide nanozyme for determination of chromium in water. *Anal. Chim. Acta* **2020**, *1117*, 9–17. [CrossRef]
97. Serebrennikova, K.V.; Komova, N.S.; Berlina, A.N.; Zherdev, A.V.; Dzantiev, B.B. Tannic Acid-Capped Gold Nanoparticles as a Novel Nanozyme for Colorimetric Determination of Pb2+ Ions. *Chemosensors* **2021**, *9*, 332. [CrossRef]
98. Liu, X.N.; Huang, L.J.; Wang, Y.P.; Sun, J.; Yue, T.L.; Zhang, W.T.; Wang, J.L. One-pot bottom-up fabrication of a 2D/2D heterojuncted nanozyme towards optimized peroxidase-like activity for sulfide ions sensing. *Sens. Actuators B-Chem.* **2020**, *306*, 127565. [CrossRef]
99. Vu, T.H.; Nguyen, P.T.; Kim, M.I. Polydopamine-Coated Co_3O_4 Nanoparticles as an Efficient Catalase Mimic for Fluorescent Detection of Sulfide Ion. *Biosensors* **2022**, *12*, 1047. [CrossRef]
100. Xue, Q.S.; Niu, X.H.; Liu, P.; Wang, M.Z.; Peng, Y.X.; Peng, H.B.; Li, X. Analyte-triggered citrate-stabilized Au nanoparticle aggregation with accelerated peroxidase-mimicking activity for catalysis-based colorimetric sensing of arsenite. *Sensors and Actuators B-Chem.* **2021**, *334*, 129650. [CrossRef]
101. Huang, H.; Li, M.N.; Hao, M.W.; Yu, L.L.; Li, Y.X. A novel selective detection method for sulfide in food systems based on the GMP-Cu nanozyme with laccase activity. *Talanta* **2021**, *235*, 122775. [CrossRef] [PubMed]
102. Zhao, Q.; Gou, W.X.; Zhang, X.T.; Zhang, M.Y.; Bu, Y.R.; Wang, L.J.; Hu, L.; Yao, W.L.; Yan, Z.Q. Hg^{2+}-activated oxidase-like activity of Ag_2S@graphene oxide nanozyme and its naked-eye monitoring Hg^{2+} application with obvious hyperchromic effect. *Appl. Surf. Sci.* **2021**, *545*, 148973. [CrossRef]
103. Luo, L.P.; Su, Z.H.; Zhuo, J.C.; Huang, L.J.; Nian, Y.; Su, L.H.; Zhang, W.T.; Wang, J.L. Copper-Sensitized "Turn On" Peroxidase-Like Activity of $MMoO_4$ (M = Co, Ni) Flowers for Selective Detection of Aquatic Copper Ions. *Acs Sustain. Chem. Eng.* **2020**, *8*, 12568–12576. [CrossRef]
104. Shi, W.; He, M.Q.; Li, W.T.; Wei, X.; Bui, B.; Chen, M.L.; Chen, W. Cu-Based Metal-Organic Framework Nanoparticles for Sensing Cr(VI) Ions. *Acs Appl. Nano Mater.* **2021**, *4*, 802–810. [CrossRef]
105. Borthakur, P.; Das, M.R.; Szunerits, S.; Boukherroub, R. CuS Decorated Functionalized Reduced Graphene Oxide: A Dual Responsive Nanozyme for Selective Detection and Photoreduction of Cr(VI) in an Aqueous Medium. *Acs Sustain. Chem. Eng.* **2019**, *7*, 16131–16143. [CrossRef]
106. Mao, Y.; Gao, S.J.; Yao, L.L.; Wang, L.; Qu, H.; Wu, Y.; Chen, Y.; Zheng, L. Single-atom nanozyme enabled fast and highly sensitive colorimetric detection of Cr(VI). *J. Hazard. Mater.* **2021**, *408*, 124898. [CrossRef] [PubMed]
107. Yi, W.W.; Zhang, P.; Wang, Y.P.; Li, Z.P.; Guo, Y.J.; Liu, M.; Dong, C.; Li, C.F. Copper ferrite nanoparticles loaded on reduced graphene oxide nanozymes for the ultrasensitive colorimetric assay of chromium ions. *Anal. Methods* **2022**, *14*, 3434–3443. [CrossRef]
108. Li, W.J.; Liu, C.; Liu, D.; Liu, S.D.; You, T.Y. Ratiometric fluorescent sensing of mercury (II) ion based on the Pt nanozyme-triggered fluorescence resonance energy transfer between Si quantum dots and 2,3-diaminophenazine. *Sens. Actuators A-Phys.* **2021**, *331*, 112976. [CrossRef]
109. Ko, E.; Hur, W.; Son, S.E.; Seong, G.H.; Han, D.K. Au nanoparticle-hydrogel nanozyme-based colorimetric detection for on-site monitoring of mercury in river water. *Microchim. Acta* **2021**, *188*, 382. [CrossRef] [PubMed]
110. Zhou, J.J.; Zhu, W.J.; Lv, X.Q.; Du, X.P.; He, J.L.; Cai, J. Dendritic Silica Nanospheres with Au-Pt Nanoparticles as Nanozymes for Label-Free Colorimetric Hg^{2+} Detection. *Acs Appl. Nano Mater.* **2022**, *5*, 18885–18893. [CrossRef]
111. Wang, C.H.; Tang, G.G.; Tan, H.L. Colorimetric determination of mercury(II) via the inhibition by ssDNA of the oxidase-like activity of a mixed valence state cerium-based metal-organic framework. *Microchim. Acta* **2018**, *185*, 475. [CrossRef] [PubMed]

112. Li, Q.; Wu, F.; Mao, M.; Ji, X.; Wei, L.Y.; Li, J.Y.; Ma, L. A dual-mode colorimetric sensor based on copper nanoparticles for the detection of mercury-(ii) ions. *Anal. Methods* **2019**, *11*, 4014–4021. [CrossRef]
113. Dai, J.W.; Wang, L.W.; Xu, F.A.; Ma, G.R. Dual-functional Fe-MoS_2@AuNPs for simple and sensitive colorimetric-electrochemical coupled detection of Hg^{2+}. *Ionics* **2022**, *28*, 5251–5255. [CrossRef]
114. Cao, L.G.; Fang, Y.M.; Zhang, Y.; Yang, J.Z.; He, J.H. Colorimetric Detection of Hg^{2+} Based on the Promotion of Oxidase-Like Catalytic Activity of Ag Nanowires. *Int. J. Nanosci.* **2020**, *19*, 2050004. [CrossRef]
115. Niu, X.H.; He, Y.F.; Li, X.; Zhao, H.L.; Pan, J.M.; Qiu, F.X.; Lan, M.B. A peroxidase-mimicking nanosensor with Hg^{2+}-triggered enzymatic activity of cysteine-decorated ferromagnetic particles for ultrasensitive Hg^{2+} detection in environmental and biological fluids. *Sens. Actuators B-Chem.* **2019**, *281*, 445–452. [CrossRef]
116. Fu, M.L.; Li, L.; Yang, D.Y.; Tu, Y.F.; Yan, J.L. Colorimetric detections of iodide and mercuric ions based on a regulation of an Enzyme-Like activity from gold nanoclusters. *Spectrochim. Acta Part A Mol. Biomol. Spectrosc.* **2022**, *279*, 121450. [CrossRef]
117. Tian, X.; Liao, H.; Wang, M.; Feng, L.Y.; Fu, W.S.; Hu, L.Z. Highly sensitive chemiluminescent sensing of intracellular Al^{3+} based on the phosphatase mimetic activity of cerium oxide nanoparticles. *Biosens. Bioelectron.* **2020**, *152*, 112027. [CrossRef]
118. Liu, H.; Hua, Y.; Cai, Y.Y.; Feng, L.P.; Li, S.; Wang, H. Mineralizing gold-silver bimetals into hemin-melamine matrix: A nanocomposite nanozyme for visual colorimetric analysis of H_2O_2 and glucose. *Anal. Chim. Acta* **2019**, *1092*, 57–65. [CrossRef]
119. Guan, H.J.; Zhao, Y.F.; Cheng, J.H.; Zhang, Y.D.; Yang, Q.; Zhang, B. Fabrication of Pt/CeO_2/NCNFs with embedded structure as high-efficiency nanozyme for electrochemical sensing of hydrogen peroxide. *Synth. Met.* **2020**, *270*, 116604. [CrossRef]
120. Lei, Y.; He, B.; Huang, S.J.; Chen, X.Y.; Sun, J. Facile Fabrication of 1-Methylimidazole/Cu Nanozyme with Enhanced Laccase Activity for Fast Degradation and Sensitive Detection of Phenol Compounds. *Molecules* **2022**, *27*, 4712. [CrossRef]
121. Adegoke, O.; Daeid, N.N. Polymeric-coated Fe-doped ceria/gold hybrid nanocomposite as an aptasensor for the catalytic enhanced colorimetric detection of 2,4-dinitrophenol. *Colloids Surf. A-Physicochem. Eng. Asp.* **2021**, *627*, 127194. [CrossRef]
122. Ma, Y.J.; Deng, M.S.; Wang, X.F.; Gao, X.H.; Song, H.X.; Zhu, Y.H.; Feng, L.Y.; Zhang, Y. 2H-MoS_2/Co_3O_4 nanohybrid with type I nitroreductase-mimicking activity for the electrochemical assays of nitroaromatic compounds. *Anal. Chim. Acta* **2022**, *1221*, 340078. [CrossRef]
123. Sun, X.; Xie, Y.; Chu, H.C.; Long, M.; Zhang, M.Y.; Wang, Y.; Hu, X.Y. A highly sensitive electrochemical biosensor for the detection of hydroquinone based on a magnetic covalent organic framework and enzyme for signal amplification. *New J. Chem.* **2022**, *46*, 11902–11909. [CrossRef]
124. Huang, H.; Lei, L.L.; Bai, J.; Zhang, L.; Song, D.H.; Zhao, J.Q.; Li, J.L.; Li, Y.X. Efficient elimination and detection of phenolic compounds in juice using laccase mimicking nanozymes. *Chin. J. Chem. Eng.* **2021**, *29*, 167–175. [CrossRef]
125. Zhu, X.; Tang, J.; Ouyang, X.L.; Liao, Y.B.; Feng, H.P.; Yu, J.F.; Chen, L.; Lu, Y.T.; Yi, Y.Y.; Tang, L. Multifunctional MnCo@C yolk-shell nanozymes with smartphone platform for rapid colorimetric analysis of total antioxidant capacity and phenolic compounds. *Biosens. Bioelectron.* **2022**, *216*, 114652. [CrossRef]
126. Omar, N.A.; Jabbar, H.S. $NiFe_2O_4$ nanoparticles as nanozymes, a new colorimetric probe for 2,4-dichlorophenoxyacetic acid herbicide detection. *Inorg. Chem. Commun.* **2022**, *146*, 110104. [CrossRef]
127. Zhu, X.Y.; Liu, P.; Ge, Y.; Wu, R.M.; Xue, T.; Sheng, Y.Y.; Ai, S.R.; Tang, K.J.; Wen, Y.P. MoS_2/MWCNTs porous nanohybrid network with oxidase-like characteristic as electrochemical nanozyme sensor coupled with machine learning for intelligent analysis of carbendazim. *J. Electroanal. Chem.* **2020**, *862*, 113940. [CrossRef]
128. Shah, M.M.; Ren, W.; Irudayaraj, J.; Sajini, A.A.; Ali, M.I.; Ahmad, B. Colorimetric Detection of Organophosphate Pesticides Based on Acetylcholinesterase and Cysteamine Capped Gold Nanoparticles as Nanozyme. *Sensors* **2021**, *21*, 8050. [CrossRef]
129. Huang, L.J.; Sun, D.W.; Pu, H.B.; Wei, Q.Y.; Luo, L.P.; Wang, J.L. A colorimetric paper sensor based on the domino reaction of acetylcholinesterase and degradable gamma-MnOOH nanozyme for sensitive detection of organophosphorus pesticides. *Sens. Actuators B-Chem.* **2019**, *290*, 573–580. [CrossRef]
130. Wu, J.H.; Yang, Q.T.; Li, Q.; Li, H.Y.; Li, F. Two-Dimensional MnO_2 Nanozyme-Mediated Homogeneous Electrochemical Detection of Organophosphate Pesticides without the Interference of H_2O_2 and Color. *Anal. Chem.* **2021**, *93*, 4084–4091. [CrossRef]
131. Xu, L.L.; Xiong, Y.; Wu, R.M.; Geng, X.; Li, M.H.; Yao, H.; Wang, X.; Wen, Y.P.; Ai, S.R. An Emerging Machine Learning Strategy for the Fabrication of Nanozyme Sensor and Voltametric Determination of Benomyl In Agro-Products. *J. Electrochem. Soc.* **2022**, *169*, 047506. [CrossRef]
132. Li, F.; Jiang, J.M.; Peng, H.; Li, C.X.; Li, B.; He, J.B. Platinum nanozyme catalyzed multichannel colorimetric sensor array for identification and detection of pesticides. *Sens. Actuators B-Chem.* **2022**, *369*, 132334. [CrossRef]
133. Zhu, X.Y.; Lin, L.; Wu, R.M.; Zhu, Y.F.; Sheng, Y.Y.; Nie, P.C.; Liu, P.; Xu, L.L.; Wen, Y.P. Portable wireless intelligent sensing of ultra-trace phytoregulator alpha-naphthalene acetic acid using self-assembled phosphorene/Ti_3C_2-MXene nanohybrid with high ambient stability on laser induced porous graphene as nanozyme flexible electrode. *Biosens. Bioelectron.* **2021**, *179*, 113062. [CrossRef] [PubMed]
134. Khairy, M.; Ayoub, H.A.; Banks, C.E. Non-enzymatic electrochemical platform for parathion pesticide sensing based on nanometer-sized nickel oxide modified screen-printed electrodes. *Food Chem.* **2018**, *255*, 104–111. [CrossRef]
135. Li, Q.L.; Li, H.; Li, K.X.; Gu, Y.; Wang, Y.J.; Yang, D.Z.; Yang, Y.L.; Gao, L. Specific colorimetric detection of methylmercury based on peroxidase-like activity regulation of carbon dots/Au NPs nanozyme. *J. Hazard. Mater.* **2023**, *441*, 129919. [CrossRef]

136. Weerathunge, P.; Behera, B.K.; Zihara, S.; Singh, M.; Prasad, S.N.; Hashmi, S.; Mariathomas, P.R.D.; Bansal, V.; Ramanathan, R. Dynamic interactions between peroxidase-mimic silver NanoZymes and chlorpyrifos-specific aptamers enable highly-specific pesticide sensing in river water. *Anal. Chim. Acta* **2019**, *1083*, 157–165. [CrossRef]
137. Song, G.C.; Zhang, J.J.; Huang, H.X.; Wang, X.; He, X.Y.; Luo, Y.B.; Li, J.C.; Huang, K.L.; Cheng, N. Single-atom Ce-N-C nanozyme bioactive paper with a 3D-printed platform for rapid detection of organophosphorus and carbamate pesticide residues. *Food Chem.* **2022**, *387*, 132896. [CrossRef] [PubMed]
138. Wei, J.C.; Yang, L.L.; Luo, M.; Wang, Y.T.; Li, P. Nanozyme-assisted technique for dual mode detection of organophosphorus pesticide. *Ecotoxicol. Environ. Saf.* **2019**, *179*, 17–23. [CrossRef] [PubMed]
139. Sun, Y.Z.; Wei, J.C.; Zou, J.; Cheng, Z.H.; Huang, Z.M.; Gu, L.Q.; Zhong, Z.F.; Li, S.L.; Wang, Y.T.; Li, P. Electrochemical detection of methyl-paraoxon based on bifunctional cerium oxide nanozyme with catalytic activity and signal amplification effect. *J. Pharm. Anal.* **2021**, *11*, 653–660. [CrossRef] [PubMed]
140. Li, S.H.; Pang, C.H.; Ma, X.H.; Zhang, Y.L.; Xu, Z.; Li, J.P.; Zhang, M.; Wang, M.Y. Microfluidic paper-based chip for parathion-methyl detection based on a double catalytic amplification strategy. *Microchim. Acta* **2021**, *188*, 438. [CrossRef] [PubMed]
141. Boruah, P.K.; Das, M.R. Dual responsive magnetic Fe_3O_4-TiO_2/graphene nanocomposite as an artificial nanozyme for the colorimetric detection and photodegradation of pesticide in an aqueous medium. *J. Hazard. Mater.* **2020**, *385*, 121516. [CrossRef]
142. Wang, Z.H.; Shu, Y.Y.; Li, J.J.; Liang, A.H.; Jiang, Z.L. Silver nanosol RRS aptamer assay of trace glyphosate based on gold-doped. *Microchem. J.* **2022**, *176*, 107252. [CrossRef]
143. Wu, Z.; Hu, Y.; Pan, X.L.; Tang, Y.; Dai, Y.F.; Wu, Y.G. A liquid colorimetric chemosensor for ultrasensitive detection of glyphosate residues in vegetables using a metal oxide with intrinsic peroxidase catalytic activity. *Food Addit. Contam. Part A Chem. Anal. Control. Expo. Risk Assess* **2022**, *39*, 710–723. [CrossRef] [PubMed]
144. Chen, D.; Wang, C.Q.; Yang, D.Z.; Deng, H.M.; Li, Q.L.; Chen, L.; Zhao, G.K.; Shi, J.L.; Zhang, K.; Yang, Y.L. A portable smartphone-based detection of glyphosate based on inhibiting peroxidase-like activity of heptanoic acid/Prussian blue decorated Fe_3O_4 nanoparticles. *RSC Adv.* **2022**, *12*, 25060–25067. [CrossRef] [PubMed]
145. Liu, P.; Li, X.; Xu, X.C.; Ye, K.; Wang, L.J.; Zhu, H.J.; Wang, M.Z.; Niu, X.H. Integrating peroxidase-mimicking activity with photoluminescence into one framework structure for high-performance ratiometric fluorescent pesticide sensing. *Sens. Actuators B-Chem.* **2021**, *328*, 129024. [CrossRef]
146. Xu, X.C.; Wu, S.W.; Guo, D.Z.; Niu, X.H. Construction of a recyclable oxidase-mimicking Fe_3O_4@MnOx-based colorimetric sensor array for quantifying and identifying chlorophenols. *Anal. Chim. Acta* **2020**, *1107*, 203–212. [CrossRef]
147. Zhang, X.; Zhou, Y.; Huang, X.; Hu, X.; Huang, X.; Yin, L.; Huang, Q.; Wen, Y.; Li, B.; Shi, J.; et al. Switchable aptamer-fueled colorimetric sensing toward agricultural fipronil exposure sensitized with affiliative metal-organic framework. *Food Chem.* **2022**, *407*, 135115. [CrossRef]
148. Ge, J.; Yang, L.K.; Li, Z.H.; Wan, Y.; Mao, D.S.; Deng, R.J.; Zhou, Q.; Yang, Y.; Tan, W.H. A colorimetric smartphone-based platform for pesticides detection using Fe-N/C single-atom nanozyme as oxidase mimetics. *J. Hazard. Mater.* **2022**, *436*, 129199. [CrossRef]
149. Xiao, J.X.; Hu, X.L.; Wang, K.; Zou, Y.M.; Gyimah, E.; Yakubu, S.; Zhang, Z. A novel signal amplification strategy based on the competitive reaction between 2D Cu-TCPP(Fe) and polyethyleneimine (PEI) in the application of an enzyme-free and ultrasensitive electrochemical immunosensor for sulfonamide detection. *Biosens. Bioelectron.* **2020**, *150*, 111883. [CrossRef]
150. Wei, D.; Zhang, X.; Chen, B.; Zeng, K. Using bimetallic Au@Pt nanozymes as a visual tag and as an enzyme mimic in enhanced sensitive lateral-flow immunoassays: Application for the detection of streptomycin. *Anal. Chim. Acta* **2020**, *1126*, 106–113. [CrossRef]
151. Shen, Y.Z.; Wei, Y.L.; Liu, Z.M.; Nie, C.; Ye, Y.W. Engineering of 2D artificial nanozyme-based blocking effect-triggered colorimetric sensor for onsite visual assay of residual tetracycline in milk. *Microchim. Acta* **2022**, *189*, 233. [CrossRef]
152. Liu, B.X.; Zhu, H.J.; Feng, R.L.; Wang, M.Z.; Hu, P.W.; Pan, J.M.; Niu, X.H. Facile molecular imprinting on magnetic nanozyme surface for highly selective colorimetric detection of tetracycline. *Sens. Actuators B Chem.* **2022**, *370*, 132451. [CrossRef]
153. Zhu, B.C.; Dong, S.M.; Liu, Z.C.; Gao, Y.; Zhu, X.X.; Xie, M.; Liu, Q.Y. Enhanced peroxidase-like activity of bimetal (Fe/Co) MIL-101 for determination of tetracycline and hydrogen peroxide. *New J. Chem.* **2022**, *46*, 21834–21844. [CrossRef]
154. Li, S.H.; Ma, X.H.; Pang, C.H.; Wang, M.Y.; Yin, G.H.; Xu, Z.; Li, J.P.; Luo, J.H. Novel chloramphenicol sensor based on aggregation-induced electrochemiluminescence and nanozyme amplification. *Biosens. Bioelectron.* **2021**, *176*, 112944. [CrossRef] [PubMed]
155. Tang, Y.; Hu, Y.; Zhou, P.; Wang, C.X.; Tao, H.; Wu, Y.G. Colorimetric Detection of Kanamycin Residue in Foods Based on the Aptamer-Enhanced Peroxidase-Mimicking Activity of Layered WS2 Nanosheets. *J. Agric. Food Chem.* **2021**, *69*, 2884–2893. [CrossRef]
156. Zhang, Z.P.; Liu, Y.; Huang, P.C.; Wu, F.Y.; Ma, L.H. Polydopamine molecularly imprinted polymer coated on a biomimetic iron-based metal-organic framework for highly selective fluorescence detection of metronidazole. *Talanta* **2021**, *232*, 122411. [CrossRef]
157. Lu, C.; Tang, L.H.; Gao, F.; Li, Y.Z.; Liu, J.W.; Zheng, J.K. DNA-encoded bimetallic Au-Pt dumbbell nanozyme for high-performance detection and eradication of *Escherichia coli* O157:H7. *Biosens. Bioelectron.* **2021**, *187*, 113327. [CrossRef]
158. Liu, J.C.; Xing, Y.P.; Xue, B.Y.; Zhou, X.H. Nanozyme enhanced paper-based biochip with a smartphone readout system for rapid detection of cyanotoxins in water. *Biosens. Bioelectron.* **2022**, *205*, 114099. [CrossRef]

159. Zhang, J.C.; Bai, Q.; Bi, X.L.; Zhang, C.H.; Shi, M.Y.; Yu, W.W.; Du, F.L.; Wang, L.A.; Wang, Z.B.; Zhu, Z.L.; et al. Piezoelectric enhanced peroxidase-like activity of metal-free sulfur doped graphdiyne nanosheets for efficient water pollutant degradation and bacterial disinfection. *Nano Today* **2022**, *43*, 101429. [CrossRef]
160. Geng, X.; Xie, X.N.; Liang, Y.C.; Li, Z.Q.; Yang, K.; Tao, J.; Zhang, H.; Wang, Z. Facile Fabrication of a Novel Copper Nanozyme for Efficient Dye Degradation. *Acs Omega* **2021**, *6*, 6284–6291. [CrossRef]
161. Chen, Q.M.; Liu, Y.; Lu, Y.W.; Hou, Y.J.; Zhang, X.D.; Shi, W.B.; Huang, Y.M. Atomically dispersed Fe/Bi dual active sites single-atom nanozymes for cascade catalysis and peroxymonosulfate activation to degrade dyes. *J. Hazard. Mater.* **2022**, *422*, 126929. [CrossRef]
162. Su, C.; Wang, B.X.; Li, S.L.; Wie, Y.B.; Wang, Q.L.; Li, D.J. Fabrication of Pd@ZnNi-MOF/GO Nanocomposite and Its Application for H_2O_2 Detection and Catalytic Degradation of Methylene Blue Dyes. *Chemistryselect* **2021**, *6*, 8480–8489. [CrossRef]
163. Zhu, J.L.; Luo, G.; Xi, X.X.; Wang, Y.J.; Selvaraj, J.N.; Wen, W.; Zhang, X.H.; Wang, S.F. Cu^{2+}-modified hollow carbon nanospheres: An unusual nanozyme with enhanced peroxidase-like activity. *Microchim. Acta* **2021**, *188*, 8. [CrossRef]
164. Shams, S.; Ahmad, W.; Memon, H.; Wei, Y.; Yuan, Q.P.; Liang, H. Facile synthesis of laccase mimic Cu/H3BTC MOF for efficient dye degradation and detection of phenolic pollutants. *RSC Adv.* **2019**, *9*, 40845–40854. [CrossRef] [PubMed]
165. Li, Z.G.; Chen, Z.M.; Zhu, Q.P.; Song, J.J.; Li, S.; Liu, X.H. Improved performance of immobilized laccase on Fe_3O_4@C-Cu^{2+} nanoparticles and its application for biodegradation of dyes. *J. Hazard. Mater.* **2020**, *399*, 123088. [CrossRef]
166. Zha, J.Q.; Wu, W.G.; Xie, P.; Han, H.H.; Fang, Z.; Chen, Y.T.; Jia, Z.F. Polymeric Nanocapsule Enhances the Peroxidase-like Activity of Fe_3O_4 Nanozyme for Removing Organic Dyes. *Catalysts* **2022**, *12*, 614. [CrossRef]
167. Su, H.F.; Zhang, Y.Z.; Lu, Z.C.; Wang, Q.Y. A mechanism of microbial sensitivity regulation on interventional remediation by nanozyme manganese oxide in soil heavy metal pollution. *J. Clean. Prod.* **2022**, *373*, 133470. [CrossRef]
168. Yan, Z.Q.; Xing, L.; Zhao, L.; Zhang, X.Y.; Zhang, Y.F.; Tang, Y.L.; Zhou, X.M.; Hu, L.; Zhu, N.L. beta-Cyclodextrin and graphene oxide co-strengthened AgRu bimetal mesoporous nanozyme: An efficient strategy for visual detection and removal of toxic Hg^{2+} and Cl. *J. Environ. Chem. Eng.* **2022**, *10*, 108242. [CrossRef]
169. Wang, F.M.; Zhang, Y.; Liu, Z.W.; Ren, J.S.; Qu, X.G. A mesoporous encapsulated nanozyme for decontaminating two kinds of wastewater and avoiding secondary pollution. *Nanoscale* **2020**, *12*, 14465–14471. [CrossRef]
170. Lv, R.; Sun, S.Y.; Wang, K.; Golubev, Y.A.; Dong, F.Q.; Kotova, O.B.; Liu, J.; Liu, M.X.; Tan, D.Y. Design and construction of copper-containing organophyllosilicates as laccase-mimicking nanozyme for efficient removal of phenolic pollutants. *J. Mater. Sci.* **2022**, *57*, 10084–10099. [CrossRef]
171. Jiang, J.F.; He, C.Y.; Wang, S.; Jiang, H.; Li, J.D.; Li, L.S. Recyclable ferromagnetic chitosan nanozyme for decomposing phenol. *Carbohydr. Polym.* **2018**, *198*, 348–353. [CrossRef] [PubMed]
172. Lin, Y.M.; Wang, F.; Yu, J.; Zhang, X.; Lu, G.P. Iron single-atom anchored N-doped carbon as a 'laccase-like' nanozyme for the degradation and detection of phenolic pollutants and adrenaline. *J. Hazard. Mater.* **2022**, *425*, 127763. [CrossRef] [PubMed]
173. Wang, J.H.; Huang, R.L.; Qi, W.; Su, R.X.; Binks, B.P.; He, Z.M. Construction of a bioinspired laccase-mimicking nanozyme for the degradation and detection of phenolic pollutants. *Appl. Catal. B Environ.* **2019**, *254*, 452–462. [CrossRef]
174. Tang, Y.; Jiang, S.L.; Li, W.Y.; Shah, S.J.; Zhao, Z.X.; Pan, L.; Zhao, Z.X. Confined construction of COF@Cu-nanozyme with high activity and stability as laccase biomimetic catalyst for the efficient degradation of phenolic pollutants. *Chem. Eng. J.* **2022**, *448*, 137701. [CrossRef]
175. Xu, X.J.; Wang, J.H.; Huang, R.L.; Qi, W.; Su, R.X.; He, Z.M. Preparation of laccase mimicking nanozymes and their catalytic oxidation of phenolic pollutants. *Catal. Sci. Technol.* **2021**, *11*, 3402–3410. [CrossRef]
176. Liang, S.; Wu, X.L.; Zong, M.H.; Lou, W.Y. Construction of Zn-heptapeptide bionanozymes with intrinsic hydrolase-like activity for degradation of di(2-ethylhexyl) phthalate. *J. Colloid Interface Sci.* **2022**, *622*, 860–870. [CrossRef] [PubMed]
177. Zandieh, M.; Liu, J.W. Removal and Degradation of Microplastics Using the Magnetic and Nanozyme Activities of Bare Iron Oxide Nanoaggregates. *Angew. Chem. Int. Ed.* **2022**, *61*, e202212013. [CrossRef]
178. Khulbe, K.; Karmakar, K.; Ghosh, S.; Chandra, K.; Chakravortty, D.; Mugesh, G. Nanoceria-Based Phospholipase-Mimetic Cell Membrane Disruptive Antibiofilm Agents. *ACS Appl. Bio Mater.* **2020**, *3*, 4316–4328. [CrossRef]
179. Fuentes, K.M.; Onna, D.; Rioual, T.; Huvelle, M.A.L.; Britto, F.; Simian, M.; Sanchez-Dominguez, M.; Soler-Illia, G.; Bilmes, S.A. Copper upcycling by hierarchical porous silica spheres functionalized with branched polyethylenimine: Antimicrobial and catalytic applications. *Microporous Mesoporous Mater.* **2021**, *327*, 111391. [CrossRef]
180. Fan, Y.F.; Gan, X.R.; Zhao, H.M.; Zeng, Z.X.; You, W.J.; Quan, X. Multiple application of SAzyme based on carbon nitride nanorod-supported Pt single-atom for H_2O_2 detection, antibiotic detection and antibacterial therapy. *Chem. Eng. J.* **2022**, *427*, 131572. [CrossRef]
181. Boruah, P.K.; Darabdhara, G.; Das, M.R. Polydopamine functionalized graphene sheets decorated with magnetic metal oxide nanoparticles as efficient nanozyme for the detection and degradation of harmful triazine pesticides. *Chemosphere* **2021**, *268*, 129328. [CrossRef]
182. Yang, D.C.; Huo, J.Q.; Zhang, Z.; An, Z.X.; Dong, H.J.; Wang, Y.N.; Duan, W.D.; Chen, L.; He, M.X.; Gao, S.T.; et al. Citric acid modified ultrasmall copper peroxide nanozyme for in situ remediation of environmental sulfonylurea herbicide contamination. *J. Hazard. Mater.* **2023**, *443*, 130265. [CrossRef] [PubMed]
183. Pan, J.; Ai, X.; Ma, C.; Zhang, G. Degradable Vinyl Polymers for Combating Marine Biofouling. *Acc. Chem. Res.* **2022**, *55*, 1586–1598. [CrossRef]

184. Dobretsov, S.; Abed, R.M.M.; Teplitski, M. Mini-review: Inhibition of biofouling by marine microorganisms. *Biofouling* **2013**, *29*, 423–441. [CrossRef] [PubMed]
185. Cao, S.; Wang, J.; Chen, H.; Chen, D. Progress of marine biofouling and antifouling technologies. *Chin. Sci. Bull.* **2011**, *56*, 598–612. [CrossRef]
186. Luo, Q.; Li, Y.; Huo, X.; Li, L.; Song, Y.; Chen, S.; Lin, H.; Wang, N. Atomic Chromium Coordinated Graphitic Carbon Nitride for Bioinspired Antibiofouling in Seawater. *Adv. Sci.* **2022**, *9*, 2105346. [CrossRef] [PubMed]
187. Wang, W.; Luo, Q.; Li, J.Y.; Li, L.Q.; Li, Y.H.; Huo, X.B.; Du, X.W.; Li, Z.S.; Wang, N. Photothermal-Amplified Single Atom Nanozyme for Biofouling Control in Seawater. *Adv. Funct. Mater.* **2022**, *32*, 2205461. [CrossRef]
188. You, J.; Chen, F.; Zhao, X.; Chen, Z. Preparation, characterization and catalytic oxidation property of CeO_2/Cu^{2+}-attapulgite (ATP) nanocomposites. *J. Rare Earths* **2010**, *28*, 347–352. [CrossRef]
189. Feng, F.; Zhang, X.; Mu, B.; Wang, P.X.; Chen, Z.S.; Zhang, J.H.; Zhang, H.F.; Zhuang, J.L.; Zhao, L.; An, Q.; et al. Attapulgite Doped with Fe and Cu Nanooxides as Peroxidase Nanozymes for Antibacterial Coatings. *ACS Appl. Nano Mater.* **2022**, *5*, 16720–16730. [CrossRef]
190. Wei, F.; Cui, X.; Wang, Z.; Dong, C.; Li, J.; Han, X. Recoverable peroxidase-like Fe_3O_4@MoS_2-Ag nanozyme with enhanced antibacterial ability. *Chem. Eng. J.* **2021**, *408*, 127240. [CrossRef]
191. Hao, S.; Sun, X.; Zhang, H.; Zhai, J.; Dong, S. Recent development of biofuel cell based self-powered biosensors. *J. Mater. Chem. B* **2020**, *8*, 3393–3407. [CrossRef]
192. Lutterbeck, C.A.; Machado, E.L.; Sanchez-Barrios, A.; Silveira, E.O.; Layton, D.; Rieger, A.; Lobo, E.A. Toxicity evaluation of hospital laundry wastewaters treated by microbial fuel cells and constructed wetlands. *Sci. Total Environ.* **2020**, *729*, 138816. [CrossRef]
193. Torres Castillo, N.E.; Melchor-Martinez, E.M.; Ochoa Sierra, J.S.; Mariana Ramirez-Torres, N.; Eduardo Sosa-Hernandez, J.; Iqbal, H.M.N.; Parra-Saldivar, R. Enzyme mimics in-focus: Redefining the catalytic attributes of artificial enzymes for renewable energy production. *Int. J. Biol. Macromol.* **2021**, *179*, 80–89. [CrossRef]
194. Le, P.G.; Kim, M.I. Research Progress and Prospects of Nanozyme-Based Glucose Biofuel Cells. *Nanomaterials* **2021**, *11*, 2116. [CrossRef]
195. Gu, C.; Kong, X.; Yan, S.; Gai, P.; Li, F. Glucose Dehydrogenase-like Nanozyme Based on Black Phosphorus Nanosheets for High-Performance Biofuel Cells. *ACS Sustain. Chem. Eng.* **2020**, *8*, 16549–16554. [CrossRef]
196. Ho, J.; Li, Y.; Dai, Y.; Kim, T.; Wang, J.; Ren, J.; Yun, H.; Liu, X. Ionothermal synthesis of N-doped carbon supported $CoMn_2O_4$ nanoparticles as ORR catalyst in direct glucose alkaline fuel cell. *Int. J. Hydrogen Energy* **2021**, *46*, 20503–20515. [CrossRef]
197. Li, Z.; Kang, Z.; Zhu, Z. A photo-switch for enzymatic biofuel cells based on the photo-oxidization of electron acceptor in cathode by C-dots nanozyme. *Chem. Eng. J.* **2022**, *428*, 13125. [CrossRef]